

1965

A critical study of the stress singularities of an elastic polygon under longitudinal shear

Walter C. Ballard
Lehigh University

Follow this and additional works at: <https://preserve.lehigh.edu/etd>



Part of the [Applied Mechanics Commons](#)

Recommended Citation

Ballard, Walter C., "A critical study of the stress singularities of an elastic polygon under longitudinal shear" (1965). *Theses and Dissertations*. 3340.
<https://preserve.lehigh.edu/etd/3340>

This Thesis is brought to you for free and open access by Lehigh Preserve. It has been accepted for inclusion in Theses and Dissertations by an authorized administrator of Lehigh Preserve. For more information, please contact preserve@lehigh.edu.

A CRITICAL STUDY OF THE STRESS
SINGULARITIES OF AN ELASTIC POLYGON
UNDER LONGITUDINAL SHEAR

by

Walter Chambers Ballard

A Thesis

Presented to the Graduate Faculty

of Lehigh University

in Candidacy for the Degree of

Master of Science

Lehigh University

1965

This thesis is accepted and approved in partial fulfillment of the requirements for the degree of Master of Science

May 11, 1965

Date

Fazıl E.doğan

Professor in Charge

Ferdinand P. Beer

Head of the Department

Table of Contents

Abstract	1
1. Introduction	2
2. Elastic Wedge	4
3. Wedge of Two Bonded Elastic Media	10
4. The Problem of Bonded Planes with a Diamond Shaped Cavity	19
5. Elastic Polygon Bonded to a Rigid Foundation	26
Examples	31
Tables	42
Figures	45
References	53
Vita	55

Abstract

The order of the stress singularity at its vertex of a wedge of two bonded elastic media under longitudinal shear is solved by use of the Williams method. The similar problem of an elastic wedge bonded to a rigid foundation is also solved using the same method. Next, the problem of a cylindrical elastic media whose boundary is a polygon bonded to a rigid foundation and subjected to various types of longitudinal shear loads on its boundary is considered. A number of examples are worked out and expressions for contact stresses along the bonds are given.

I. Introduction

In the field of fracture mechanics considerable attention has recently been given to the evaluation of stress singularities in elastic materials (for survey and ref. see, Irwin [1], Barenblatt [2] and Sneddon [3]). Most of the work in this field deals with the determination of the stress state in the vicinity of cracks in homogeneous media. Williams [4,5] has studied the form of the stress singularity in bonded dissimilar planes containing semi-infinite cracks. The solution of the general problem of two bonded semi-infinite dissimilar planes containing a series of cracks along the bond has been solved by Erdogan [6,7].

Barenblatt and Cherepanov [8] have considered the infinite homogeneous plane containing cracks of various geometries and subjected to longitudinal shear. Erdogan [9] has recently solved the problem of two semi-infinite elastic media bonded along $y=0$ plane, containing cracks or symmetric cavities with surfaces parallel to the z -axis and subjected to longitudinal shear forces or tractions in various ways. In the first part of this thesis we study the form of the stress singularity at the crack-tip in the problem solved by Erdogan [9]. In particular, we solve the problem of the stress singularity at its vertex of a wedge of two bonded

elastic media under longitudinal shear using a technique similar to that developed by Williams [4]. This solution is then checked against [9].

Next we consider the problem of a 3-dimensional cylindrical elastic media whose boundary is a polygon bonded to a rigid foundation and subjected to various types of longitudinal shear loads on its boundary. For example, consider a block of aluminum bonded to a foundation made of steel. The elastic shear modulus of aluminum is much smaller than that of steel; therefore, the deformations in the steel foundation are negligible compared to the deformations in the aluminum block so that for all practical purposes the steel foundation may be considered rigid. This problem can also be applied to three-dimensional cylindrical polycrystalline materials with different properties containing cavities or cracks along the crystal boundaries and subjected to various types of longitudinal shear loads.

2. Elastic Wedge

Consider an infinite elastic wedge with its generators parallel to the z-direction (Fig. 1) and external loads and displacements parallel to the z-axis and independent of the z-coordinate. Following [8], for the displacements and stresses we have

$$u = 0, \quad v = 0, \quad w = w(x, y) \quad (1)$$

$$\sigma_x = \sigma_y = \sigma_z = \tau_{xy} = 0, \quad \tau_{yz} = \mu \frac{\partial w}{\partial y}, \quad \tau_{xz} = \mu \frac{\partial w}{\partial x}$$

where μ is the shear modulus. Substituting (1) into the equilibrium equations yields

$$\nabla^2 w = 0 \quad (2)$$

From [4] we see that around the wedge tip w may be written in polar coordinates as the product solution of a function of r and θ ($0 < \theta < m\pi$).

$$w = r^\lambda F(\theta) \quad (3)$$

In polar coordinates (2) becomes

$$r^2 \frac{\partial^2 w}{\partial r^2} + r \frac{\partial w}{\partial r} + \frac{\partial^2 w}{\partial \theta^2} = 0 \quad (4)$$

Substituting (3) into (4) yields,

$$F''(\theta) + \lambda^2 F(\theta) = 0 \quad (5)$$

where the primes represent differentiation with respect to θ . Solving the differential equation (5) for $F(\theta)$ yields

$$F(\theta) = A_n \cos \lambda_n \theta + B_n \sin \lambda_n \theta \quad (6)$$

where A_n and B_n are constants determined from the boundary conditions. Substituting (6) into (3) yields

$$w = r^{\lambda_n} (A_n \cos \lambda_n \theta + B_n \sin \lambda_n \theta) \quad (7)$$

In polar coordinates τ_{yz} and τ_{xz} are replaced by $\tau_{\theta z}$ and τ_{rz} and the latter two are given by

$$\tau_{rz} = \mu \frac{\partial w}{\partial r} \quad (8)$$

$$\tau_{\theta z} = \frac{\mu}{r} \frac{\partial w}{\partial \theta} \quad (9)$$

Differentiating (7) with respect to θ and r and substituting into (8) and (9) yields

$$\tau_{rz} = \mu \lambda_n r^{\lambda_n - 1} (A_n \cos \lambda_n \theta + B_n \sin \lambda_n \theta) \quad (10)$$

$$\tau_{\theta z} = \mu \lambda_n r^{\lambda_n - 1} (-A_n \sin \lambda_n \theta + B_n \cos \lambda_n \theta) \quad (11)$$

Case I - Clamped-Free Wedge

Consider the case where the edge, $\theta = m\pi$, is stress free and the edge, $\theta = 0$, is clamped. Substituting $\theta = 0$ in (7) and $\theta = m\pi$ in (11) and setting them equal to zero yields

$$\tau_{\theta} (m\pi) = 0 = -\mu \lambda_n r^{\lambda_n - 1} (-A_n \sin \lambda_n m\pi + B_n \cos \lambda_n m\pi) \quad (12)$$

$$w(0) = 0 = A_n r^{\lambda_n} \quad (13)$$

From (12) and (13) we have

$$A_n = 0 \quad (14)$$

$$\cos \lambda_n m\pi = 0$$

which implies

$$m\pi \lambda_n = \left(\frac{2n-1}{2}\right)\pi \quad n = 1, 2, 3, \dots \quad (15)$$

$$\lambda_n = \frac{2n-1}{2m} \quad n = 1, 2, 3, \dots \quad (16)$$

Near the wedge tip, that is for small values of r the displacement and stresses may be expressed as

$$w = r^{1/2m} (B_1 \sin \frac{\theta}{2m}) + O(r^{3/2m})$$

$$\tau_{\theta z} = \left(\frac{\mu}{2m}\right) r^{\frac{1-2m}{2m}} (B_1 \cos \frac{\theta}{2m}) + O(r^{\frac{3-2m}{2m}})$$

$$\tau_{rz} = \left(\frac{\mu}{2m}\right) r^{\frac{1-2m}{2m}} (B_1 \sin \frac{\theta}{2m}) + O(r^{\frac{3-2m}{2m}})$$

From the last equation the order of the stress singularity at the wedge tip is given by $r^{\frac{1-2m}{2m}}$. Define

$$\lambda^* = \frac{1-2m}{2m} \tag{18}$$

Equation (18) shows the following analogies:

$$m < \frac{1}{2}, \lambda^* > 0; \quad m > \frac{1}{2}, \lambda^* < 0; \quad m = \frac{1}{2}, \lambda^* = 0$$

The results show that for the clamped-free case there are stress singularities at the wedge tip only for $m > \frac{1}{2}$.

Case II, Free-Free

Consider the case where the edges, $\theta = m\pi$ and $\theta = 0$ are stress free. Substituting $\theta = 0$ and $\theta = m\pi$ in (11)

and setting the resulting expressions equal to zero yields

$$0 = \mu \lambda_n r^{\lambda_n - 1} (0 + B_n) \quad (19)$$

$$0 = \mu \lambda_n r^{\lambda_n - 1} (-A_n \sin \lambda_n m \pi + B_n \cos \lambda_n m \pi) \quad (20)$$

If we take the determinant of the coefficients of A_n and B_n in (19) and (20) and set them equal to zero we have

$$\sin \lambda_n m \pi = 0 \quad (21)$$

$$B_n = 0$$

which implies

$$m \pi \lambda_n = n \pi \quad n = 1, 2, 3, \dots \quad (22)$$

$$\lambda_n = \frac{n}{m} \quad n = 1, 2, 3, \dots \quad (23)$$

Again, for small values of r the stresses become

$$\tau_{\theta z} = \left(\frac{\mu}{m}\right) r^{\frac{1-m}{m}} \left(-A_1 \sin \frac{\theta}{m}\right) + O\left(r^{\frac{2-m}{m}}\right) \quad (24)$$

$$\tau_{rz} = \left(\frac{\mu}{m}\right) r^{\frac{1-m}{m}} \left(A_1 \cos \frac{\theta}{m}\right) + O\left(r^{\frac{2-m}{m}}\right)$$

Equation (24) shows that there are no singularities at the vertex except for $m > 1$.

Case III - Clamped - Clamped

If the edges $\theta = m$ and $\theta = 0$ are clamped, equation (7) at these values of θ becomes

$$0 = r^{\lambda_n} (A_n + 0) \quad (25)$$

$$0 = r^{\lambda_n} (A_n \cos \lambda_n m \pi + B_n \sin \lambda_n m \pi) \quad (26)$$

from which we have

$$A_n = 0 \quad (27)$$

$$\sin \lambda_n m \pi = 0$$

It then follows that

$$\tau_{\theta z} = \frac{\mu}{m} r^{\frac{1-m}{m}} (B_1 \cos \frac{\theta}{m}) + O(r^{\frac{2-m}{m}})$$

$$\tau_{rz} = \frac{\mu}{m} r^{\frac{1-m}{m}} (B_1 \sin \frac{\theta}{m}) + O(r^{\frac{2-m}{m}})$$

It is obvious that equations (22) and (23) from case II follow and that the results for the order of stress singularity in both case II and case III are the same.

3. Wedge of Two Bonded Elastic Media

Consider an infinite wedge of two bonded elastic media with its generators parallel to the z -direction (Fig. 2) and external loads and displacements parallel to the z -axis and independent of the z -coordinate.

Now let two elastic media with shear moduli μ_1 and μ_2 occupy the lower and upper portions of the wedge S^- and S^+ , respectively (Fig. 2). Let the two media be bonded along the strip L on the real axis x . w_1 and w_2 will have to satisfy (1) in S^- and S^+ and following [9] the boundary conditions may be written as

$$w_1^-(t) - w_2^+(t) = h(t) \quad \text{on } L \quad (28)$$

$$\tau_{1yz}^-(t) = \tau_{2yz}^+(t) \quad \text{on } L \quad (29)$$

where the subscripts 1 and 2 refer to lower and upper parts of the wedge, t is the coordinate along the real axis, and $h(t)$ is the dislocation along the bonds.

Let

$$w_1 = r^\lambda F_1(\theta) \quad (30)$$

$$w_2 = r^\lambda F_2(\theta) \quad (31)$$

Substituting (30) and (31) into (4) yields two differential equations in $F_1(\theta)$ and $F_2(\theta)$ identical to (5) whose solutions are identical to (6); therefore, we have

$$F_1(\theta) = A_n \cos \lambda_n \theta + B_n \sin \lambda_n \theta \quad (32)$$

$$F_2(\theta) = C_n \cos \lambda_n \theta + D_n \sin \lambda_n \theta \quad (33)$$

In polar coordinates we replace τ_{1yz} and τ_{2yz} by $\tau_{1\theta z}$ and $\tau_{2\theta z}$. Equation (29) becomes

$$\tau_{1\theta z}^-(0) = \tau_{2\theta z}^+(0) \quad (34)$$

From (8) and (9) we have

$$\tau_{j\theta z} = \frac{\mu_j}{r} \frac{\partial w_j}{\partial \theta} \quad j = 1, 2 \quad (35)$$

$$\tau_{jr z} = \mu_j \frac{\partial w_j}{\partial r} \quad j = 1, 2 \quad (36)$$

Substituting (30) - (33) into (35) yields

$$\tau_{1\theta z} = \mu_1 r^{\lambda-1} \lambda_n (-A_n \sin \lambda_n \theta + B_n \cos \lambda_n \theta) \quad (37)$$

$$\tau_{2\theta z} = \mu_2 r^{\lambda-1} \lambda_n (-C_n \sin \lambda_n \theta + D_n \cos \lambda_n \theta) \quad (38)$$

If we substitute (37) and (38) into (34), we have

$$D_n = \frac{\mu_1}{\mu_2} B_n \quad (39)$$

Case I - Mixed Boundary Conditions

Consider the case for which the dislocation along the bond line L is zero and the edges are stress free. We then have

$$h(t) = 0 \quad (40)$$

$$\tau_{2\theta z}(m\pi) = \tau_{1\theta z}(-k\pi) = 0$$

$$\text{from (28), } 0 = A_n + 0 - C_n \quad (41)$$

$$\text{from (37), } 0 = A_n \sin k\pi\lambda_n + B_n \cos k\pi\lambda_n + 0 \quad (42)$$

$$\text{from (38), } 0 = 0 + B_n \frac{\mu_1}{\mu_2} \cos m\pi\lambda_n - C_n \sin m\pi\lambda_n \quad (43)$$

In order for A_n , B_n , and C_n not all to be identically zero, the determinant of their coefficients must be zero which yields

$$\cos k\pi\lambda_n \sin m\pi\lambda_n + \frac{\mu_1}{\mu_2} \sin k\pi\lambda_n \cos m\pi\lambda_n = 0 \quad (44)$$

Equation (44) is then the eigen-equation from which λ_n must be determined: Dividing (44) by $\cos k\pi\lambda_n \cos m\pi\lambda_n$ yields

$$\tan m\pi\lambda_n = - \left(\frac{\mu_1}{\mu_2} \right) \tan k\pi\lambda_n \quad (45)$$

Define:

$$\alpha = \frac{\mu_1}{\mu_2} \quad (46)$$

$$x = k\pi\lambda_n \quad (47)$$

$$\beta = \frac{m}{k} \quad (48)$$

Substituting (46), (47), and (48) into (45) reduces (45) to

$$\tan \beta x = -\alpha \tan x \quad (49)$$

Next, we choose eleven values of α and β . We then construct an eleven by eleven matrix with each member of the matrix representing the first value of x such that $0 < x < \pi$ which satisfies equation (49) for the corresponding value of α and β . The results are shown in table I and the graph in Fig. 17. Once x is known, the smallest value of λ between 0 and 1 is determined from equation (47) as a function of k . Equation (48) is then used to calculate m once k is stipulated.

Case II

Consider the case where the dislocation along the bond line is zero and the displacements on the edges are also zero. Applying the boundary conditions yields

$$\text{from (28), } 0 = A_n - C_n \quad (50)$$

$$\text{from (30), } 0 = A_n \cos k\pi\lambda_n - B_n \sin k\pi\lambda_n \quad (51)$$

$$\text{from (31), } 0 = \frac{\mu_1}{\mu_2} B_n \sin m\pi\lambda_n + C_n \cos m\pi\lambda_n \quad (52)$$

If we take the determinant of the coefficients of A_n , B_n , and C_n in (50), (51) and (52) and set it equal to zero, we have

$$\frac{\mu_1}{\mu_2} \cos k\pi\lambda_n \sin m\pi\lambda_n + \sin k\pi\lambda_n \cos m\pi\lambda_n = 0 \quad (53)$$

Equation (53) reduces to

$$\frac{\mu_1}{\mu_2} \tan m\pi\lambda_n = - \tan k\pi\lambda_n \quad (54)$$

Substituting (46), (47) and (48) into (54) yields

$$\alpha \tan \beta x = - \tan x \quad (55)$$

As in case I we form an eleven by eleven matrix and calculate the first value of x between 0 and π from equation (49) for given values of α and β . The results are shown in Table II and the graph in Fig. 18.

Case III

Consider the case for which the edges are stress free and the derivative of the dislocation is zero along the bond line. Differentiating (28) with respect to t yields

$$\bar{w}_1'(t) - \bar{w}_2'(t) = h'(t) \quad (56)$$

In polar coordinates the t axis is equal to r and from (36) we see that (56) becomes

$$\frac{\tau_{1rz}^-(r)}{\mu_1} - \frac{\tau_{2rz}^+(r)}{\mu_2} = h'(t) \quad (57)$$

Applying the boundary conditions yields

$$\text{from (57), } \frac{A_n}{\mu_1} - \frac{C_n}{\mu_2} = 0 \quad (58)$$

$$\text{from (37), } A_n \sin k\pi\lambda_n + B_n \cos k\pi\lambda_n = 0 \quad (59)$$

$$\text{from (38), } B_n \frac{\mu_1}{\mu_2} \cos m\pi\lambda_n - C_n \sin m\pi\lambda_n = 0 \quad (60)$$

If we take the determinant of the coefficients of the constants in equations (58) to (60) and set it equal to zero, we have the following eigen-equation for λ_n .

$$\frac{\mu_1}{\mu_2} \sin k\pi\lambda_n \cos m\pi\lambda_n + \frac{\mu_2}{\mu_1} \cos k\pi\lambda_n \sin m\pi\lambda_n = 0 \quad (61)$$

Equation (61) reduces to

$$\left(\frac{\mu_1}{\mu_2}\right)^2 \tan k\pi\lambda_n = \tan m\pi\lambda_n \quad (62)$$

If we substitute equations (46) - (48) into (62), we have

$$- \alpha^2 \tan x = \tan \beta x \quad (63)$$

Again, as in case I and II we form an eleven by eleven matrix and determine the first value of x between 0 and π satisfying equation (63) for the given values of α and β . The results are shown in Table III and the graph in Fig. 19.

There are several interesting comparisons to be made between the eigen-equations for the bi-material wedge and the wedge of constant shear modulus; for example, if k or m equals zero, the bi-material wedge becomes a wedge of constant shear modulus and equations (44), (53) and (61) reduce to (21) and (27) which is as we would expect.

If the bi-material wedge is symmetric, i.e. $k=m$, equations (44), (53), and (61) reduce to

$$\sin k\pi\lambda_n \cos k\pi\lambda_n = 0. \quad (64)$$

If we recall the trigonometric identity, $\sin 2x = 2 \sin x \cos x$ equation (64) becomes

$$\sin 2k\pi\lambda_n = 0 \quad (65)$$

which implies

$$2k\pi\lambda_n = n\pi, \quad n = 1, 2, \dots \quad (66)$$

For the smallest value of λ_n between 0 and 1 we have

$$\lambda_1 = \frac{1}{2k} \quad (67)$$

Equation (66) is the same as equation (22) where the wedge angle $2\pi k$ in (66) is equal to the wedge angle $m\pi$ in (22).

If μ_1 equals μ_2 , equations (44), (53) and (61) reduce

$$\sin k\pi\lambda_n \cos m\pi\lambda_n + \cos k\pi\lambda_n \sin m\pi\lambda_n = 0 \quad (68)$$

If we recall the trigonometric identity

$$\sin (x+y) = \sin x \cos y + \sin y \cos x,$$

equation (68) becomes

$$\sin \pi\lambda_n (k+m) = 0 \quad (69)$$

which implies

$$\pi\lambda_n (k+m) = n\pi, \quad n = 1, 2, \dots \quad (70)$$

Again, for the smallest value of λ between zero and one we have

$$\lambda_1 = \frac{1}{(k+m)} \quad (71)$$

Equation (70) is the same as equation (22) where the wedge angle $(k+m)\pi$ in (70) is equal to the wedge angle $m\pi$ in (22).

4. The Problem of Bonded Planes with a Diamond-Shaped Cavity

Consider infinitely long two-bonded semi-infinite cylindrical elastic media (Figure 3) with their generators parallel to the σ direction. Let the uniform shear load q (per unit thickness) and displacements be parallel to the σ -axis and independent of the σ coordinate. Let the two media be bonded along the strip Γ on the real axis r . Let γ represent the cavity with square profile. Let the two media with the elastic shear moduli μ_1 and μ_2 occupy the lower and upper-half planes Σ^- and Σ^+ respectively. Let the sides of the square be of length a .

Assume an analytic function $\eta = \omega(\zeta)$ is found which conformally maps the Σ plane onto the S plane (Figure 4) in such a way that Σ^+ , Σ^- , γ^+ , γ^- , Γ are mapped onto S^+ , S^- , L'^+ , L'^- , L and $\omega(\zeta) \rightarrow \zeta$ as $\zeta \rightarrow \infty$. The displacements w_1 and w_2 , which are harmonic functions in $\eta = r+is$ plane, will remain harmonic in $\zeta = x+iy$ plane and the function $\omega(\zeta)$ will have a branch cut along L' . If we now consider the "equivalent longitudinal shear" problem in the ζ -plane (Figure 4), it is seen that, since $\omega(\zeta) = \zeta$ as $\zeta \rightarrow \infty$, we have

$$\tau_{kyz}^{\infty} = \tau_{kso}^{\infty} = q \quad (k=1,2)$$

In Figure 4 let the bonded media contain a central crack $(-b, b)$, the stress state at infinity q and the dislocation on L $h(t)$ be zero and the shear stress on the crack surface be $g(t) = 0$. The solution for the contact stresses along L for this problem is given by Erdogan [9] as

$$\bar{\tau}_{1yz}(t) = \frac{q t}{\sqrt{t^2 - b^2}} \quad (t > b) \quad (72)$$

Again from Erdogan [9] the contact stresses on Γ are obtained as

$$\bar{\tau}_{1s\sigma}(r) = \bar{\tau}_{1yz}(t) \frac{1}{|\omega'(t)|} \quad (73)$$

where $\bar{\tau}_{1yz}(t)$ is the equivalent shear obtained from (72). The problem now is to find a mapping function which conformally maps the square cavity in Figure 3 onto the crack in Figure 4. Consider the following Swartz-Christoffel mapping function

$$\omega'(\zeta) = \frac{d\eta}{d\zeta} = \frac{K\zeta^{1/2}}{(\zeta^2 - b^2)^{1/4}} \quad (74)$$

$$\omega(\zeta) = \eta = K \int \frac{\zeta^{1/2} d\zeta}{(\zeta^2 - b^2)^{1/4}} + L \quad (75)$$

which maps the square cavity in Figure 3 onto the crack in Figure 4. By choosing $k=1$, $\frac{dn}{d\zeta} \rightarrow 1$ as $\zeta \rightarrow \infty$. We choose b such that

$$n(D) - n(C) = \int_0^b \frac{\zeta^{1/2} d\zeta}{(\zeta^2 - b^2)^{1/4}}$$

or

$$\frac{a}{\sqrt{2}}(1-i) = \int_0^b \frac{\zeta^{1/2} d\zeta}{(\zeta^2 - b^2)^{1/4}}$$

but

$$(\zeta^2 - b^2)^{-1/4} = [e^{i\pi}(b^2 - \zeta^2)]^{-1/4} = e^{-i\pi/4}(b^2 - \zeta^2)^{-1/4}$$

$$(\zeta^2 - b^2)^{-1/4} = \frac{1}{\sqrt{2}}(1-i)(b^2 - \zeta^2)^{-1/4}$$

therefore

$$\int_0^b \frac{\zeta^{1/2} d\zeta}{(b^2 - \zeta^2)^{1/4}} = a \quad (76)$$

If we let $\zeta = b \sin \theta$, $d\zeta = b \cos \theta d\theta$, equation (76)

becomes

$$a = \int_0^{\pi/2} \frac{\sqrt{b \sin \theta} b \cos \theta d\theta}{\sqrt{b \cos \theta}}$$

$$a = b \int_0^{\pi/2} \sqrt{\sin \theta \cos \theta} d\theta$$

$$a = \frac{b}{\sqrt{2}} \int_0^{\pi/2} \sqrt{\sin 2\theta} \, d\theta$$

$$a = \frac{2b}{\sqrt{2}} \int_0^{\pi} \sqrt{\sin \theta} \, d\theta = \frac{b}{\sqrt{2}} \int_0^{\pi/2} \sqrt{\sin \theta} \, d\theta$$

$$a = \frac{b}{2} \sqrt{\frac{\pi}{2}} \frac{\Gamma(\frac{3}{4})}{\Gamma(\frac{5}{4})}$$

or

$$b = 2a \sqrt{\frac{2}{\pi}} \frac{\Gamma(\frac{5}{4})}{\Gamma(\frac{3}{4})} \quad (77)$$

The function $\omega(\zeta) \zeta \epsilon s^+$ is holomorphic except for

$\bar{\omega}(\zeta) \zeta \epsilon s^-$
 $-b < \zeta < b$; however, the value of $\omega'(\zeta)$ is well defined
for $\zeta > b$ and $\zeta < -b$.

The contact stresses are given by (73). For $|t| > b$
where t is the real axis on L

$$|\omega'(t)| = \left| \frac{t^{1/2}}{(t^2 - b^2)^{1/4}} \right| = \frac{|t|^{1/2}}{(t^2 - b^2)^{1/4}} \quad (78)$$

Hence, from (73)

$$\tau_{1s\sigma}^-(r) = \frac{qt}{\sqrt{t^2 - b^2}} \frac{(t^2 - b^2)^{-1/4}}{|t|^{1/2}}, \quad t > b$$

$$\tau_{1s\sigma}^-(r) = \frac{qt^{1/2}}{(t^2-b^2)^{1/4}} \quad t > b, \quad r = \omega(t)$$

$$\frac{\tau_{1s\sigma}^-(r)}{q} = \frac{\sqrt{\epsilon}}{(t^2-b^2)^{1/4}} \quad (79)$$

Let $t = b + \epsilon$ where ϵ is very small. Equation (79) becomes

$$\frac{\tau_{1s\sigma}^-}{q} = \frac{\sqrt{\epsilon}}{[(t-b)(t+b)]^{1/4}} = \frac{\sqrt{b}}{(2b)^{1/4} \epsilon^{1/4}}$$

or

$$\frac{\tau_{1s\sigma}^-}{q} = \left(\frac{b}{2}\right)^{1/4} \epsilon^{-1/4} \quad (80)$$

so that as $\epsilon \rightarrow 0$ the order of stress singularity at the point $t=b$ in the ζ -plane is $1/4$.

From (74) we have

$$\omega'(t) = \frac{t^{1/2}}{(t^2-b^2)^{1/4}}$$

thus for $t = (b+\epsilon)$

$$\omega'(t) = \frac{\sqrt{b}}{(2b)^{1/4} \epsilon^{1/4}} = \left(\frac{b}{2}\right)^{1/4} \epsilon^{-1/4}$$

or

$$r = \omega(t) = \frac{4}{3} \left(\frac{b}{2}\right)^{1/4} \epsilon^{3/4} + \text{constant}$$

now, as $\epsilon \rightarrow 0$, $r \rightarrow \frac{a}{\sqrt{2}}$; therefore the constant = $\frac{a}{\sqrt{2}}$. Hence, define

$$\delta = r - \frac{a}{\sqrt{2}} = \frac{4}{3} \left(\frac{b}{2}\right)^{1/4} \epsilon^{3/4}$$

therefore,

$$\epsilon^{-1/4} = \left[\frac{4}{3} \left(\frac{b}{2}\right)^{1/4}\right]^{-1/3} \delta^{-1/3} \quad (81)$$

substituting (81) into (80) gives for the stress concentration on the r axis near the point $r = \frac{a}{\sqrt{2}}$

$$\frac{\tau_{1s\sigma}(r)}{q} = \left(\frac{2b}{3}\right)^{1/3} \delta^{-1/3} \quad (82)$$

where $b = \frac{3}{\sqrt{2\pi}} (0.99706)a$, so that as $\delta \rightarrow 0$ the order of stress singularity at the point $r = \frac{a}{\sqrt{2}}$ in the n -plane is $1/3$.

Consider the case of the bi-material wedge symmetric about the bond line with mixed boundary conditions.

Equation (67) gives $\lambda_1 = \frac{1}{2k}$ where $2k$ is the wedge angle.

Since we are interested in the stress singularities, we

want to consider $\lambda_1 - 1$.

$$\lambda_1 - 1 = \frac{1}{2k} - 1 \quad (83)$$

For $k = 3/4$ (83) becomes

$$(\lambda_1 - 1) = \frac{1}{2(3/4)} - 1 = \frac{2}{3} - 1$$

$$(\lambda_1 - 1) = -\frac{1}{3} \quad (84)$$

The order of stress singularity given by (84) is the same as that given by (82) which is to be expected since both have the same wedge angle.

5. Elastic Polygon-Bonded to a Rigid Foundation

Consider an infinitely long cylindrical elastic body (Figure 5) with its generators parallel to the σ direction. Let the specified external loads and displacements be parallel to the σ axis and independent of the σ coordinate. On the surface γ with outward normal n in the r - s plane, the shear stress acting in the σ direction on γ may be written as

$$\tau_{n\sigma} = \mu \frac{\partial w}{\partial n} \quad (86)$$

Then, after [8], for the displacement and stresses we have

$$u = 0, \quad v = 0, \quad w = w(s, r) \quad (87)$$

$$\sigma_r = \sigma_s = \sigma_\sigma = \tau_{rs} = 0, \quad \tau_{s\sigma} = \mu \frac{\partial w}{\partial s}, \quad \tau_{r\sigma} = \mu \frac{\partial w}{\partial r}$$

where μ is the shear modulus. If we substitute (87) into the equilibrium equations, we obtain

$$\nabla^2 w = 0 \quad (88)$$

From (87) and (88) it is easily verified that the displacement and the stresses may be represented in terms of a single analytic function $f(\eta)$ as follows

$$w = \operatorname{Re} f(\eta), \quad \tau = \tau_{r\sigma} + i \tau_{s\sigma} = \mu \overline{f'(\eta)} \quad (89)$$

where $\eta = r + is$

The longitudinal shear problem may be formulated as follows:

$$\begin{aligned} \nabla^2 w(r,s) &= 0 && \text{in } \Sigma^+ \\ w^+(r) &= h(r) && \text{on } \Gamma \end{aligned} \quad (90)$$

$$\mu \frac{\partial w}{\partial n} = \tau_{n\sigma}^+ = q(r,s) \quad \text{on } \gamma$$

where Σ^+ is the region in the upper half of the n plane bounded by the surface γ ; Γ is the bond between the polygon and the rigid foundation; $h(r)$ is the dislocation along the bond; and $q(r,s)$ represents the resultant longitudinal shear force on γ .

Assume that an analytic function $n = \omega(\zeta)$ is found which conformally maps the Σ^+ plane (Figure 5) into the S^+ plane (Figure 6) in such a way that Σ^+ , Γ , γ are mapped onto S^+ , L , L' , and normals on γ are mapped onto normals on L' with $\omega(\zeta) \rightarrow \zeta$ as $\zeta \rightarrow \infty$. The displacement, which is a harmonic function in the n -plane, will remain harmonic in the ζ -plane.

Using the definition of directional derivative equation (90) in the ζ -plane becomes

$$\nabla^2 w(x,y) = 0 \quad \text{in } S$$

$$[\tau_{yz}(t) \left| \frac{d\zeta}{dn} \right|^+] = g(t) \quad \text{on } L' \quad (91)$$

$$w^+(t) = h(t) \quad \text{on } L$$

where t is the real axis.

Differentiating the last equation with respect to t and recalling that $\frac{dn}{d\zeta} = \omega'(\zeta)$, (91) becomes

$$\nabla^2 w(x,y) = 0 \quad \text{in } S$$

$$\tau_{yz}^+(t) = g(t) |\omega'(t)| \quad \text{on } L' \quad (92)$$

$$w'^+(t) = h'(t) \quad \text{on } L$$

For the substitute shear problem in the ζ plane equations (87) and (89) can be written as

$$\tau_{xz} = \mu \frac{\partial w}{\partial x}, \quad \tau_{yz} = \mu \frac{\partial w}{\partial y} \quad (93)$$

$$w = \text{Re } f(\zeta), \quad \tau = \tau_{xz} + i \tau_{yz} = \mu \overline{f'(\zeta)} \quad (94)$$

Defining

$$F(\zeta) = f'(\zeta) \quad (95)$$

From (94) we may write

$$w = \frac{1}{2} [f(\zeta) + \overline{f(\zeta)}]$$

(96)

$$\tau_{yz} = \frac{1}{2} \mu i [F(\zeta) - \overline{F(\zeta)}]$$

Now we define a new function $\Omega(\zeta)$ by expanding the definition of F into the lower-half plane S^- (Figure 6) as follows

$$\Omega(\zeta) = \begin{cases} F(\zeta) & \zeta \text{ in } S^+ \\ \overline{F(\zeta)} & \zeta \text{ in } S^- \end{cases} \quad (97)$$

Noting that

$$F^-(t) = F^+(t) = \Omega^-(t)$$

$$F^+(t) = \overline{F^-(t)} = \Omega^+(t)$$

and using (96) and (97), the last two equations in (92) become

$$\Omega^+(t) + \Omega^-(t) = 2h'(t) \quad \text{on } L \quad (98)$$

$$\Omega^+(t) - \Omega^-(t) = \frac{2q(t) |\omega'(t)|}{\mu i} \quad \text{on } L'$$

Thus the problem reduces to solving the Hilbert problem given by (98) to obtain the function $\Omega(\zeta)$ which is sectionally holomorphic in the entire plane. If the bond L has finite end points $(-b, a)$, the solution of (98)

may be written as [10]

$$\begin{aligned} \Omega(\zeta) = & P(\zeta) R(\zeta) + \frac{R(\zeta)}{2\pi i} \int_L \frac{2h'(t) dt}{R(t)(t-\zeta)} \\ & + \frac{R(\zeta)}{2\pi i} \int_L \frac{2q(t)|\omega'(t)| dt}{\mu i(t-\zeta) R(t)} \end{aligned} \quad (99)$$

where $P(\zeta)$ is an arbitrary polynomial consistent with the behavior of $\Omega(\zeta)$ at infinity and the sectionally holomorphic function $R(\zeta)$ is the solution of the homogeneous Hilbert problem obtained from (98) given by

$$R(\zeta) = \frac{1}{\sqrt{(\zeta+b)(\zeta-a)}} \quad (100)$$

Since L is finite $P(\zeta) = A_1 \zeta$. From the boundary conditions $\Omega(\zeta) \rightarrow 0$ as $\zeta \rightarrow \infty$ which implies that $A_1 = 0$; therefore,

$$P(\zeta) = 0 \quad (101)$$

The contact stresses on Γ are obtained as

$$\begin{aligned} \tau_{s\sigma}(r) &= \mu \frac{\partial w}{\partial s} = \mu \frac{\partial w}{\partial y} \left| \frac{dz}{dn} \right| \\ \tau_{s\sigma}(r) &= \frac{\tau_{yz}(t)}{|\omega'(t)|} \end{aligned} \quad (102)$$

Now, $\tau_{yz}(t)$ is given by

$$\tau_{yz}(t) = \frac{i\mu}{2} [\Omega^+(t) - \Omega^-(t)] \quad (103)$$

Examples

Problem 1

Consider a wedge with vertex angle $m\pi$ clamped from $r=0$ to $r=a$ under a concentrated longitudinal shear force T (per unit thickness) at the point $be^{im\pi}$ in the η -plane (Figure 7) and $\tau=0$ on the real axis for $r>a$. The mapping function is given by

$$\eta = \omega(\zeta) = \zeta^m$$

$\omega(\zeta)$ is a sectionally holomorphic function and its derivative is given by

$$\frac{d\eta}{d\zeta} = \omega'(\zeta) = \left(\frac{1}{m}\right) \zeta^{m-1} \quad (104)$$

From the boundary conditions (Figure 8) we have

$$h'(t) = 0$$

$$q(t) = T \delta(t+b^{1/m}) \quad (105)$$

$$R(\zeta) = \frac{1}{\sqrt{\zeta(\zeta-a)^{1/m}}}$$

Substituting (104) and (105) into (99) yields

$$\Omega(\zeta) = - \frac{1}{\pi\mu\sqrt{\zeta(\zeta-a^{1/m})}} \int_{L'} \frac{T\delta(t+b^{1/m})|mt^{m-1}|\sqrt{t(t-a^{1/m})}}{(t-\zeta)} dt$$

$$\bar{\Omega}(\zeta) = \frac{Tmb \frac{2m-1}{2m} \sqrt{b^{1/m}+a^{1/m}}}{\pi\mu\sqrt{\zeta(\zeta-a^{1/m})}(b^{1/m}+\zeta^{1/m})} \quad (106)$$

Substituting equations (106), (104), and (103) into equation (102), gives the contact stresses on r (Figure 7) as

$$\tau_{s\sigma}(r) = \frac{Tb \frac{2m-1}{2m} r \frac{1-2m}{2m} \sqrt{b^{1/m}+a^{1/m}}}{\pi \sqrt{a^{1/m}-r^{1/m}}(b^{1/m}+r^{1/m})} \quad (107)$$

where t has been replaced by $r^{1/m}$. From equation (107) we see that the stress singularity at $r=0$ depends on the power of r which is equal to λ^* given by equation (18); thus, the order of stress singularity obtained in equation (107) is the same as that obtained using the Williams method. For $m=1$ it is easily verified that $\tau_{s\sigma}(r)$ reduces to $\tau_{yz}(t)$ where $r=t$. Let us check the stress singularity at $r=a$. Let

$$\delta = (a-r)$$

or

$$r^{1/m} = (a-\delta)^{1/m} = a^{1/m} \left(1 - \frac{\delta}{a}\right)^{1/m}$$

The binomial expansion of $\left(1 - \frac{\delta}{a}\right)^{1/m}$ is

$$\left(1 - \frac{\delta}{a}\right)^{1/m} = 1 - \frac{\delta}{ma} + \frac{1}{m} \frac{\left(\frac{1}{m} - 1\right)}{2!} \left(\frac{\delta}{a}\right)^2 - \dots$$

Now $\delta \ll a$; therefore, we have

$$\left(1 - \frac{\delta}{a}\right)^{1/m} = 1 - \frac{\delta}{ma} + O(\delta)^2$$

hence

$$\sqrt{a^{1/m} - r^{1/m}} = \sqrt{\frac{\delta a^{1-1/m}}{m}}$$

Substituting the above equations into (107) we have

$$\tau_{s\sigma}(r) = \frac{T b^{\frac{2m-1}{2m}} a^{\frac{1-2m}{2m}}}{\pi \sqrt{\frac{\delta a^{1/m-1}}{m}} \sqrt{b^{1/m} + a^{1/m}}}$$

From the last equation we see that as $\delta \rightarrow 0$ which is equivalent to $r \rightarrow a$, $\tau_{s\sigma}(r)$ has a singularity on the order of $\frac{1}{2}$. This agrees with λ^* given by equation (18) when $m=1$.

Next consider the wedge clamped along the entire r axis, i.e., let $a \rightarrow \infty$ in equation (107) which yields

$$\tau_{s\sigma}(r) = \frac{T b^{\frac{2m-1}{2m}} r^{\frac{1-2m}{2m}}}{\pi (b^{1/m} + r^{1/m})} \quad (108)$$

Problem 2

Consider a semi-infinite rectangle (Figure 9) clamped from $r=-a$ to $r=+a$ under a concentrated shear force T (per unit thickness) at the point $n_0 = a+ib$ in the n -plane. The mapping function is given by

$$n = \omega(\zeta) = \frac{2a}{\pi} \sin^{-1} \zeta \quad (109)$$

$$\omega'(\zeta) = \frac{2a}{\pi} \left(\frac{1}{\sqrt{1-\zeta^2}} \right)$$

From the boundary conditions (Figure 10) we have

$$h'(t) = 0$$

$$q(t) = T\delta(t-c)$$

$$R(\zeta) = \frac{1}{\sqrt{\zeta^2-1}} \quad (110)$$

where

$$c = \sin \frac{\pi}{2a} (a+ib) = \cos \frac{ib\pi}{2a} = \cosh \frac{b\pi}{2a} \quad (111)$$

Substituting equations (109) and (110) into (99) yields

$$\Omega(\zeta) = - \frac{1}{\pi\mu \sqrt{\zeta^2-1}} \int_{L'} \frac{T \delta(t-c) \left| \frac{1}{\sqrt{1-t^2}} \right| \frac{2a}{\pi} \sqrt{t^2-1} dt}{(t-z)}$$

$$\Omega(\zeta) = \frac{T \cdot 2a}{\pi^2 \mu \sqrt{\zeta^2 - 1} (\zeta - c)} \quad (112)$$

Substituting equations (112), (111), (109) and (103) into (102) gives the contact stresses on Γ (Figure 9) as

$$\tau_{s\sigma}(r) = \frac{T}{\pi \left(\sin \frac{\pi r}{2a} - \cosh \frac{b\pi}{2a} \right)} \quad (113)$$

If we treat equation (112) as a Green's function and replace T by a distributed load q_0 (per unit thickness), integrating equation (112) with respect to c between the limits α and β (Figure 12) yields

$$\Omega(\zeta) = \frac{q_0 \cdot 2a}{\pi^2 \mu \sqrt{\zeta^2 - 1}} \log \left(\frac{\beta - \zeta}{\alpha - \zeta} \right) \quad (114)$$

where

$$\begin{aligned} \beta &= \cosh \frac{c\pi}{2a} \\ \alpha &= \cosh \frac{b\pi}{2a} \end{aligned} \quad \begin{array}{l} \text{Figure (11)} \\ (115) \end{array}$$

Substituting equations (115), (114), (109) and (103) into (102) gives the contact stress on Γ (Figure II) as

$$\tau_{s\sigma}(r) = \frac{q_0}{\pi \mu} \ln \left[\frac{\cosh \frac{b\pi}{2a} - \sin \frac{\pi r}{2a}}{\cosh \frac{c\pi}{2a} - \sin \frac{\pi r}{2a}} \right] \quad (116)$$

Equations (116) and (113) show that there are no stress singularities at $r = a$. In these expressions we see that $\frac{1}{(r+a)}$ is raised to the zero power which agrees with equation (18) for $m = \frac{1}{2}$ (Figure 1).

Problem 3

Consider a rectangular block bonded to a rigid foundation along r subjected to a longitudinal shear force (per unit length) T (Figure 13) at the point $n = n_0$. The mapping function is given by

$$\frac{dn}{d\zeta} = w'(\zeta) = \frac{1}{\sqrt{(\zeta^2-1)(\zeta^2-a^2)}} \quad (117)$$

$$n = - \int_0^\zeta \frac{d\zeta}{\sqrt{(\zeta^2-1)(\zeta^2-a^2)}} = - \frac{F\left(\frac{1}{a}, \sin^{-1} \zeta\right)}{a}$$

where $F(k, \phi)$ is an elliptic integral of the first kind and b and c (Figure 13) are given in terms of a (Figure 14) by

$$b = \int_0^1 \frac{dt}{\sqrt{(1-t^2)(a^2-t^2)}}$$

$$c = \int_1^a \frac{dt}{\sqrt{(t^2-1)(a^2-t^2)}}$$

To adjust the size, orientation, and position of the rectangle let $W = An + B$, where A and B are constants.

From the boundary conditions (Figure 14) we have

$$h'(t) = 0$$

$$q(t) = T\delta(t-t_0) \quad (118)$$

$$R(\zeta) = \frac{1}{\sqrt{\zeta^2-1}}$$

where ζ and t_0 (Figure 14) are given in terms of n and n_0 (Figure 13) by

$$\zeta = -\text{sn} \left[n a F \left(\frac{1}{a}, \frac{\pi}{2} \right) \right]$$

$$t_0 = -\text{sn} \left[n_0 a F \left(\frac{1}{a}, \frac{\pi}{2} \right) \right] \quad (119)$$

$$n_0 = r + ic \quad \text{or} \quad n_0 = *b + is$$

where $\text{sn}(x)$ is the Jacobian elliptic function.

Substituting equations (117) and (118) into equation (99) yields

$$\Omega(\zeta) = -\frac{1}{\sqrt{\zeta^2-1}\pi\mu} \int_L T\delta(t-t_0) \left| \frac{1}{\sqrt{(t^2-1)(t^2-a^2)}} \right| \frac{\sqrt{t^2-1} dt}{(t-\zeta)}$$

$$\Omega(\zeta) = -\frac{T}{\sqrt{\zeta^2-1}\pi\mu} \left| \frac{1}{\sqrt{t_0^2-a^2}} \right| \frac{1}{(t_0-\zeta)} \quad (120)$$

The position of t_0 with respect to a depends on n_0 in the following way: if $n_0 = r + ic$ then $|t_0| > a$; if $n_0 = \pm b + is$ then $|t_0| < a$. Substituting equations (120), (119), (117) and (103) into equation (102) gives the contact stress in the n -plane (Figure 13) as

$$\tau_{s\sigma}(r) = \left(\frac{T}{\pi}\right) \left| \frac{1}{\operatorname{sn}[n_0 a F(\frac{1}{a}, \frac{\pi}{2})] - \operatorname{sn}[ra F(\frac{1}{a}, \frac{\pi}{2})]} \right| \sqrt{\frac{a^2 - \operatorname{sn}^2[ra F(\frac{1}{a}, \frac{\pi}{2})]}{\operatorname{sn}^2[n_0 a F(\frac{1}{a}, \frac{\pi}{2})] - a^2}} \quad (121)$$

Problem 4

Consider an isosceles right triangular wedge (Figure 15) clamped from $0 < r < a$ under a concentrated shear force T (per unit thickness) at the point $n = n_0$ in the n -plane. The mapping function is given by

$$\omega(\zeta) = n = e^{\frac{3\pi i}{4}} \int_0^\zeta \frac{dt}{(t^2-1)^{3/4} t^{1/2}} \quad (122)$$

$$\omega'(\zeta) = \frac{1}{(\zeta^2-1)^{3/4} \zeta^{1/2}}$$

In Figure 15 b is given by

$$b = \int_0^1 \frac{dt}{(1-t^2)^{3/4} t^{1/2}} = \frac{B(1/4, 1/4)}{2}$$

where B equals the beta function and t is the real axis in Figure 16. From the boundary conditions (Figure 16) we have

$$h'(t) = 0$$

$$q(t) = T\delta(t-t_0) \quad (123)$$

$$R(\zeta) = \frac{1}{\sqrt{\zeta(\zeta-1)}}$$

where t_0 in Figure 16 is given such that

$$\eta_0 = e^{\frac{3\pi i}{4}} \int_0^{t_0} \frac{dt}{(t^2-1)^{3/4} t^{1/2}}$$

To adjust the size, orientation, and position of the isosceles right triangle, let $W = An + B$ where A and B are constants.

Substituting equations (123) and (122) into equation (99) yields

$$\Omega(\zeta) = - \frac{1}{\pi\mu} \frac{1}{\sqrt{\zeta(\zeta-1)}} \int_L \frac{T\delta(t-t_0) \sqrt{t(t-1)}}{(t-\zeta)(t^2-1)^{3/4} t^{1/2}} \quad (124)$$

$$\Omega(\zeta) = - \left(\frac{1}{\pi\mu \sqrt{\zeta(\zeta-1)}} \right) \left(\frac{T \sqrt{t_0-1}}{(t_0-\zeta)(t_0^2-1)^{3/4}} \right)$$

Substituting equation (124) into equation (103) gives the contact stress in the ζ -plane (Figure 16) as

$$\tau_{yz}(t) = \frac{T}{\pi} \frac{\sqrt{t_0-1}}{\sqrt{t(1-t)}(t_0-t)|t_0^2-1|^{3/4}} \quad (125)$$

From equation (102) we see that

$$\tau_{s\sigma}(r) = \frac{|1-t|^{1/4}|1+t|^{3/4} T}{\pi(t_0-t)|t_0+1|^{3/4}|t_0-1|^{1/4}} \quad (126)$$

let $t = 1 + \epsilon$ where $\epsilon \ll 1$. Equation (126) becomes

$$\tau_{s\sigma}(r) = \frac{(\epsilon)^{1/4}(2)^{3/4}T}{\pi(t_0-1)|t_0+1|^{3/4}|t_0-1|^{1/4}} \quad (127)$$

From (122) we have

$$\omega'(t) = \frac{1}{(t^2-1)^{3/4}(t)^{1/2}}$$

thus for $t = 1 + \epsilon$

$$\omega'(t) = \frac{1}{(2\epsilon)^{3/4}}$$

$$r = \omega(t) = \frac{4(\epsilon)^{1/4}}{(2)^{3/4}} + \text{const.} \quad (128)$$

As $\epsilon \rightarrow 0$, $\omega(\epsilon) \rightarrow b$; therefore, the const. = b . Define

$$\delta = r - b = \frac{4(\epsilon)^{1/4}}{(2)^{3/4}} \quad (129)$$

Substituting for $(\epsilon)^{1/4}$ in equation (127) from equation (129) yields

$$\frac{\tau_{s\sigma}(r)}{T} = \frac{\delta(2)^{3/2}}{4\pi(t_0-1)|t_0+1|^{3/4}|t_0-1|^{1/4}} \quad (130)$$

where t_0 in terms of n_0 is given by

$$n_0 = e^{\frac{3\pi i}{4}} \int_0^{t_0} \frac{dt}{(t^2-1)^{3/4} t^{1/2}}$$

From equation (130) we see that δ is raised to the first power. If we consider the case of the elastic wedge with mixed boundary conditions, we see that from equation (18), for $m = 1/4$, $\lambda^* = 1$ which agrees with the power of δ in equation (130).

$\alpha \backslash \beta$	0.2	0.4	0.6	0.8	1.0	1.2	1.5	2.0	2.5	4.0	8.0
0.1	1.82653	1.69439	1.63741	1.60065	1.57080	1.54208	1.49215	1.35594	1.16513	0.76163	0.38759
0.3	2.15005	1.88094	1.74287	1.64800	1.57080	1.50066	1.39817	1.22421	1.06002	0.72095	0.37788
0.5	2.34863	2.01741	1.82349	1.68400	1.57080	1.47203	1.34004	1.15026	0.99437	0.68792	0.36883
0.6	2.42169	2.07325	1.85729	1.69898	1.57080	1.46075	1.31811	1.12296	0.96928	0.67372	0.36456
0.7	2.48285	2.12288	1.88771	1.71238	1.57080	1.45095	1.29942	1.09983	0.94771	0.66080	0.36045
0.75	2.50983	2.14571	1.90183	1.71857	1.57080	1.44652	1.29105	1.08952	0.93800	0.65478	0.35845
0.80	2.53476	2.16736	1.91529	1.72445	1.57080	1.44236	1.28325	1.07991	0.92890	0.64902	0.35650
0.85	2.55786	2.18793	1.92185	1.73005	1.57080	1.43845	1.27596	1.07093	0.92037	0.64351	0.35458
0.90	2.57933	2.20751	1.94044	1.73538	1.57080	1.43476	1.26911	1.06252	0.91233	0.63823	0.35271
0.95	2.59932	2.22618	1.95221	1.74047	1.57080	1.43128	1.26269	1.05463	0.90475	0.63317	0.35086
1.00	2.61799	2.24399	1.96349	1.74532	1.57080	1.42799	1.25663	1.04719	0.89759	0.62831	0.34906

Table I

$\alpha \backslash \beta$	0.2	0.4	0.6	0.8	1.0	1.2	1.5	2.0	2.5	4.0	8.0
0.1	3.07118	2.91283	2.42680	1.91824	1.57080	1.32950	1.08257	0.83091	0.67775	0.44444	0.24407
0.3	2.94387	2.65006	2.23416	1.85445	1.57080	1.36191	1.13881	0.90183	0.75237	0.51464	0.29395
0.5	2.83355	2.48594	2.12149	1.81110	1.57080	1.38646	1.18191	0.95531	0.80696	0.56079	0.31961
0.6	2.78411	2.42322	2.07966	1.79416	1.57080	1.39664	1.19988	0.97759	0.82930	0.57848	0.32817
0.7	2.73812	2.36928	2.04418	1.77951	1.57080	1.40573	1.21623	0.99759	0.84915	0.59362	0.33501
0.75	2.71632	2.34500	2.02836	1.77289	1.57080	1.40992	1.22377	1.00685	0.85828	0.60041	0.33792
0.80	2.69527	2.3226	2.01362	1.76669	1.57080	1.41390	1.23095	1.01567	0.86694	0.60674	0.34057
0.85	2.67495	2.30092	1.99986	1.76086	1.57080	1.41768	1.23781	1.02409	0.87517	0.61266	0.34298
0.90	2.65531	2.28083	1.98697	1.75538	1.57080	1.42128	1.24436	1.03213	0.88300	0.61820	0.34518
0.95	2.63634	2.26189	1.97487	1.75021	1.57080	1.42472	1.25063	1.03982	0.89047	0.62341	0.34720
1.00	2.61799	2.24399	1.96349	1.74532	1.57080	1.42799	1.25663	1.04719	0.89759	0.62831	0.34906

Table II

$\alpha \backslash \beta$	0.2	0.4	0.6	0.8	1.0	1.2	1.5	2.0	2.5	4.0	8.0
0.1	1.60094	1.58440	1.58097	1.57401	1.57080	1.56758	1.56108	1.50037	1.24480	0.78291	0.39218
0.3	1.80483	1.68316	1.63124	1.59789	1.57080	1.54465	1.49857	1.36618	1.17238	0.76389	0.38810
0.5	2.08467	1.84007	1.71928	1.63743	1.57080	1.50952	1.41707	1.24904	1.08117	0.73033	0.38024
0.6	2.21891	1.92601	1.76918	1.65979	1.57080	1.49104	1.37818	1.19844	1.03756	0.71032	0.37509
0.7	2.34053	2.01143	1.81990	1.68241	1.57080	1.47325	1.34244	1.15327	0.99711	0.68942	0.36927
0.75	2.39585	2.05310	1.84504	1.69356	1.57080	1.46479	1.32591	1.13264	0.97823	0.67888	0.36614
0.80	2.44741	2.09378	1.86983	1.70451	1.57080	1.45667	1.31029	1.11327	0.96028	0.66841	0.36289
0.85	2.49526	2.13331	1.89415	1.71521	1.57080	1.44892	1.29558	1.09510	0.94326	0.65806	0.35955
0.90	2.53952	2.17156	1.91791	1.72559	1.57080	1.44156	1.28175	1.07807	0.92715	0.64790	0.35611
0.95	2.58036	2.20847	1.94104	1.73564	1.57080	1.43458	1.26878	1.06212	0.91194	0.63797	0.35261
1.00	2.61799	2.24399	1.96349	1.74532	1.57080	1.42799	1.25663	1.04719	0.89759	0.62831	0.34906

Table III

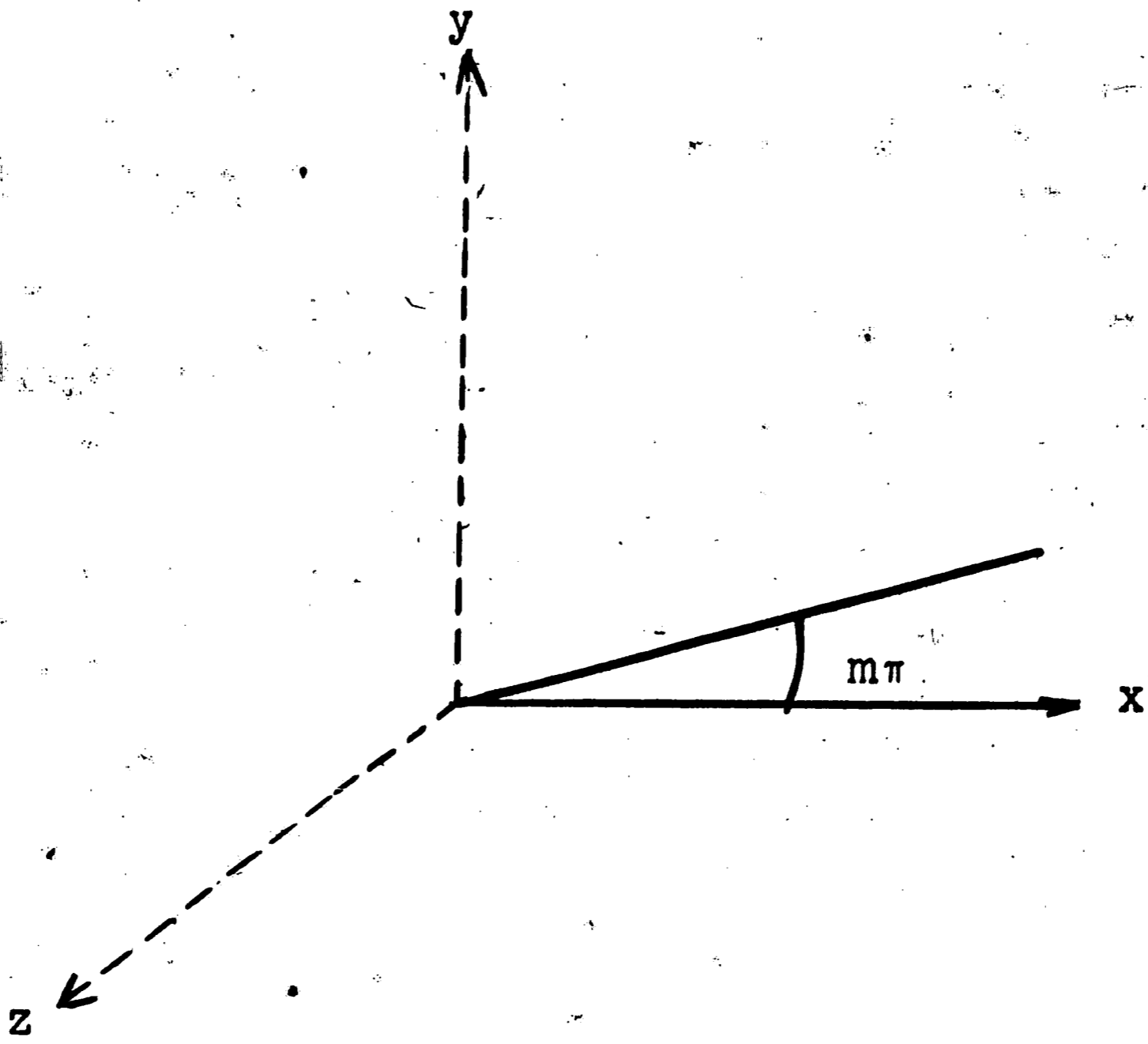


Fig. 1

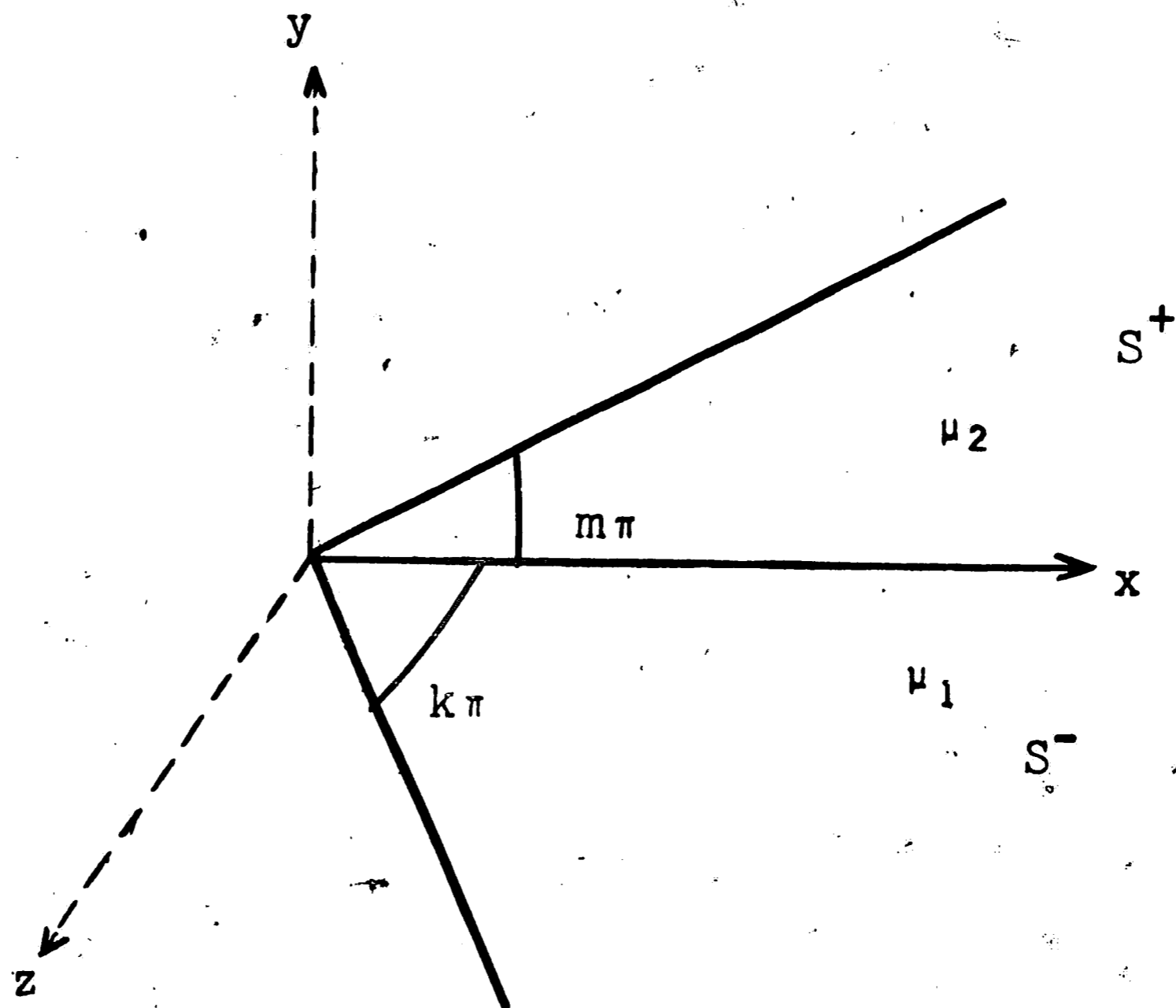


Fig. 2

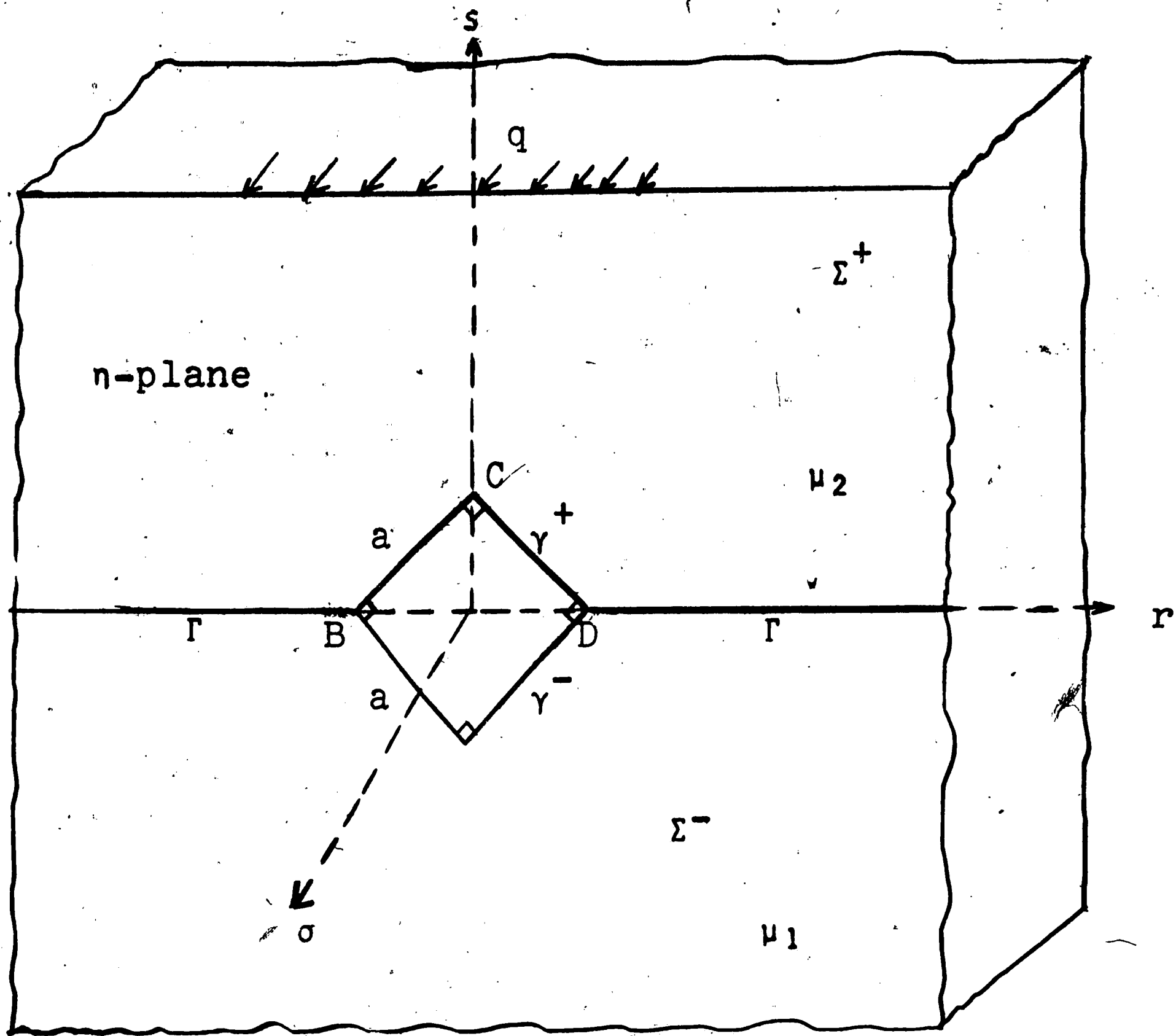


Fig. 3

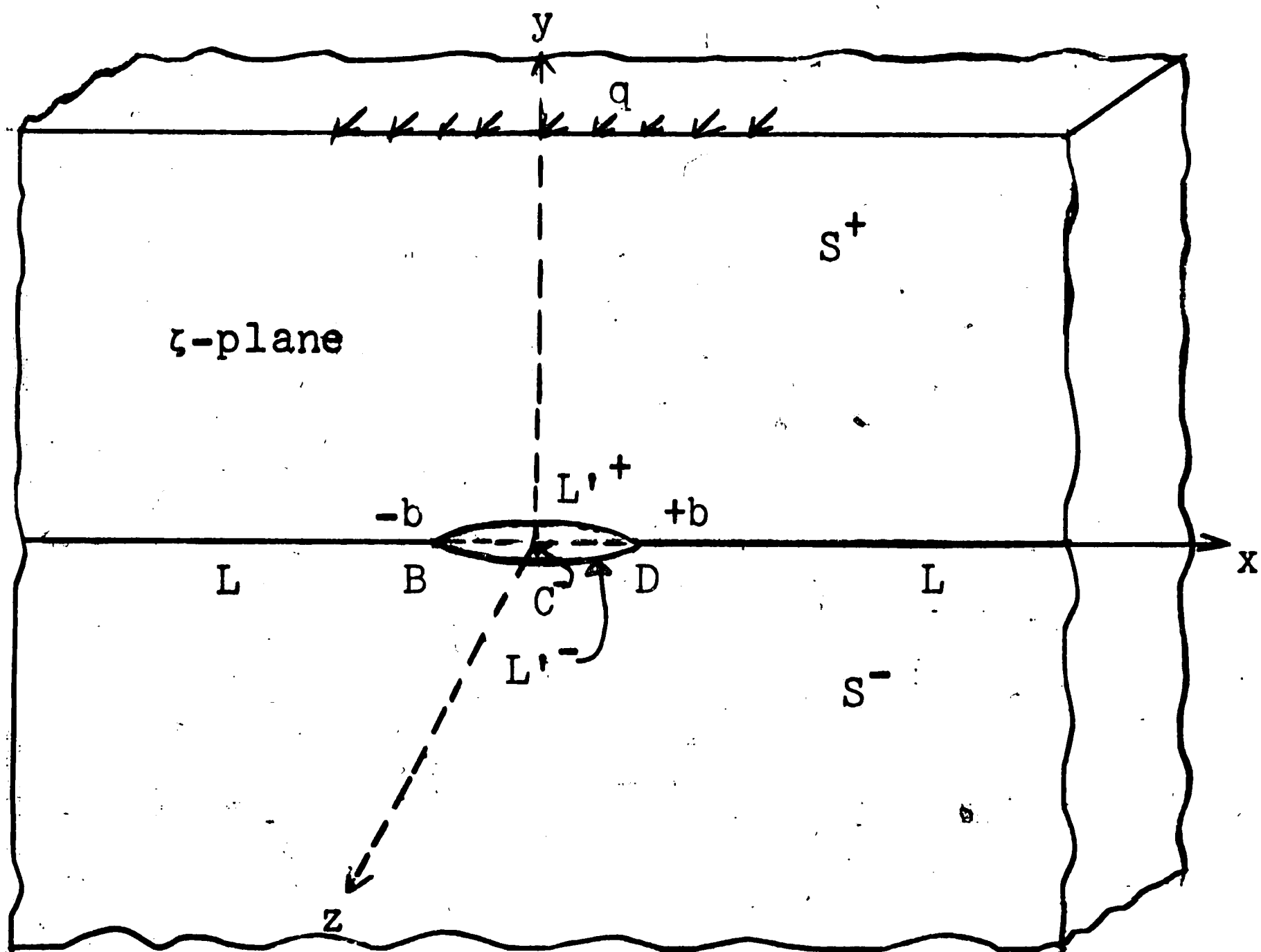


Fig. 4

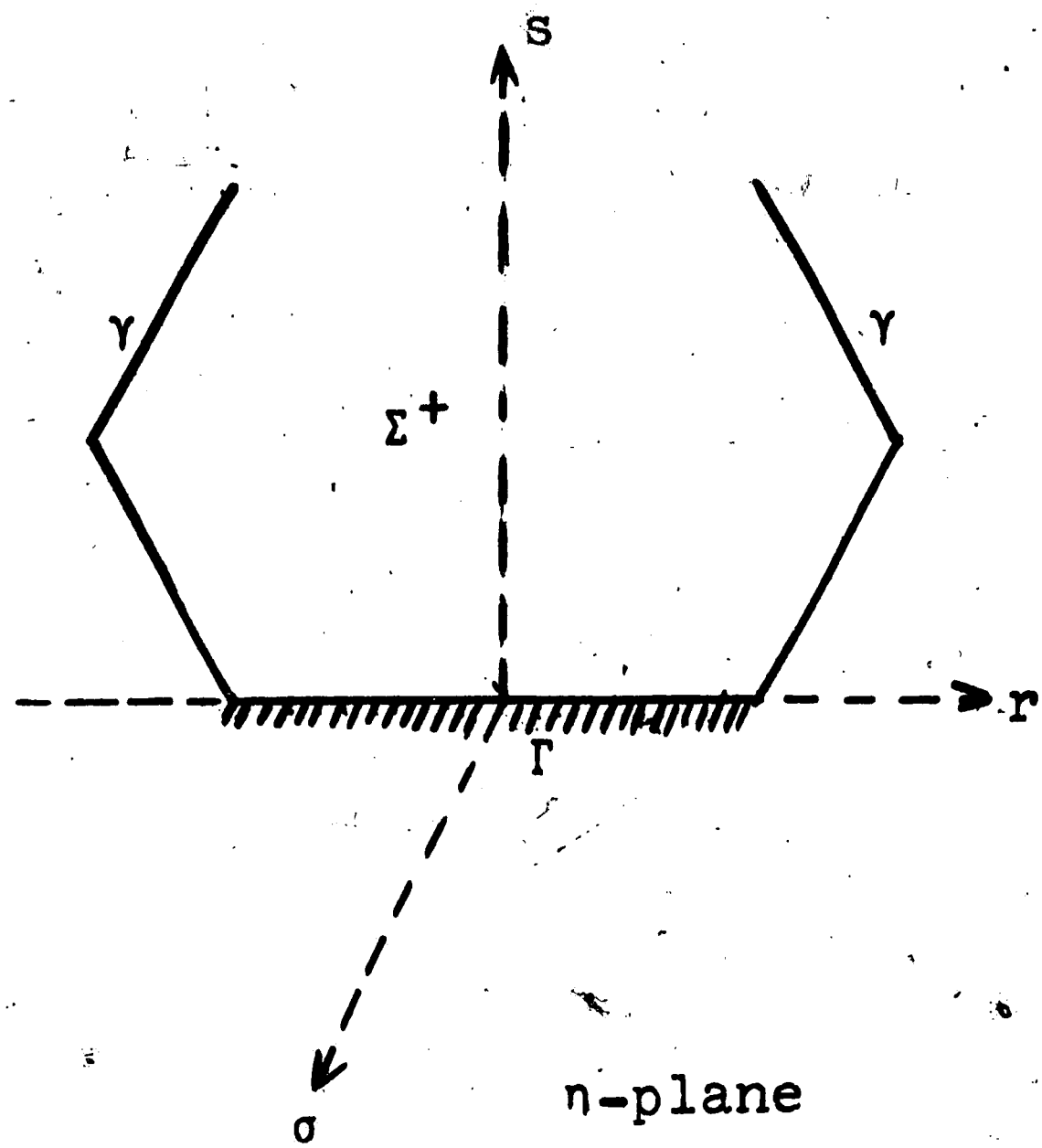


Fig. 5

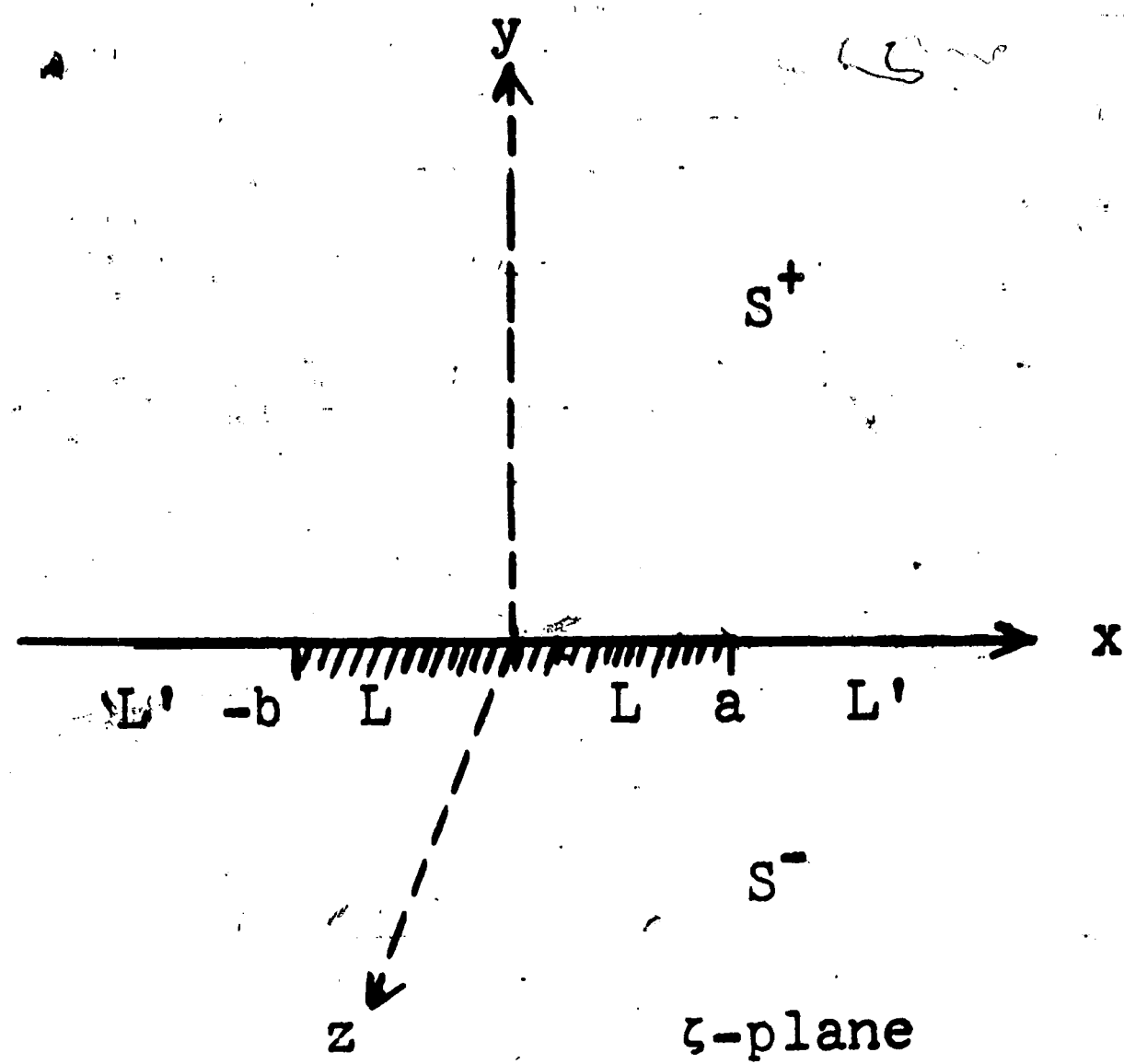


Fig. 6

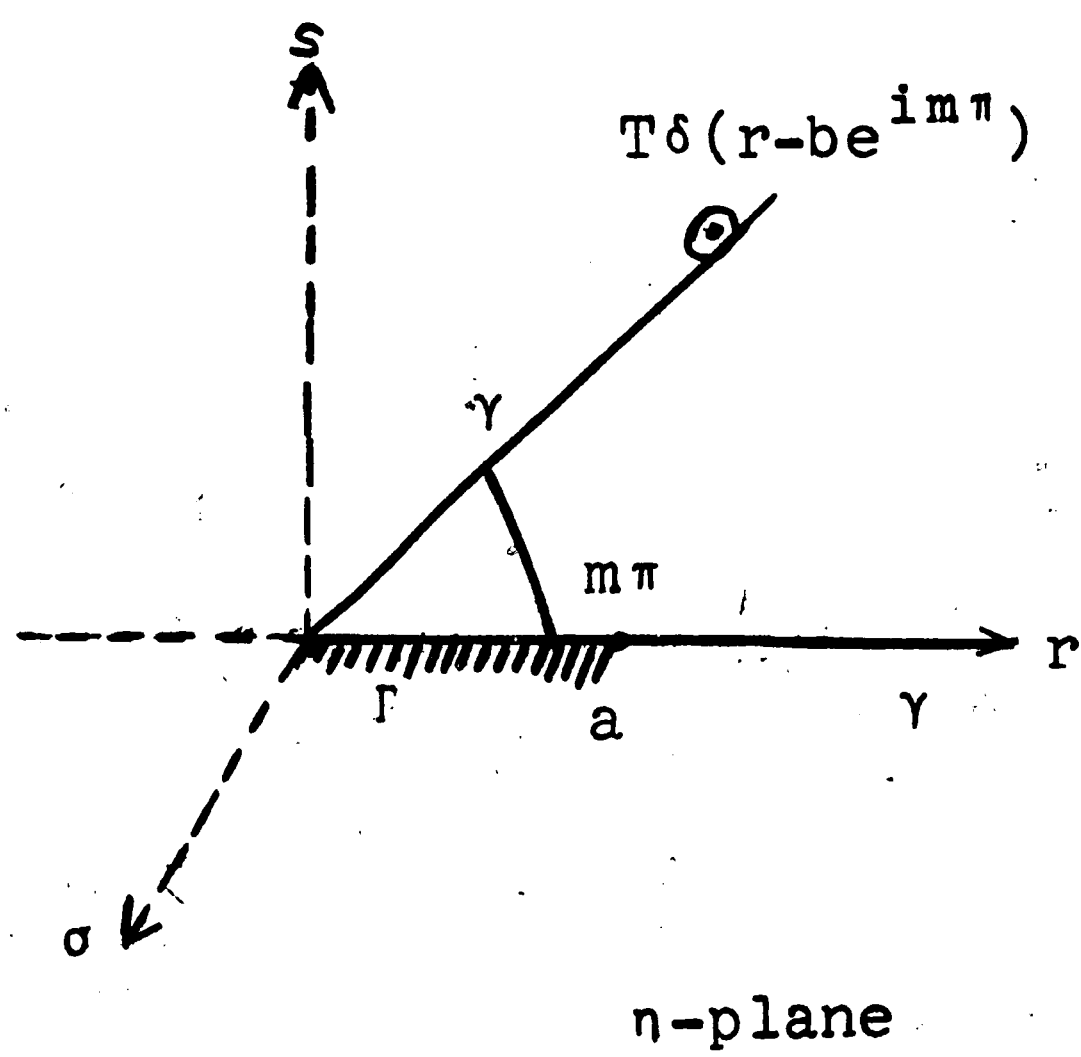


Fig. 7

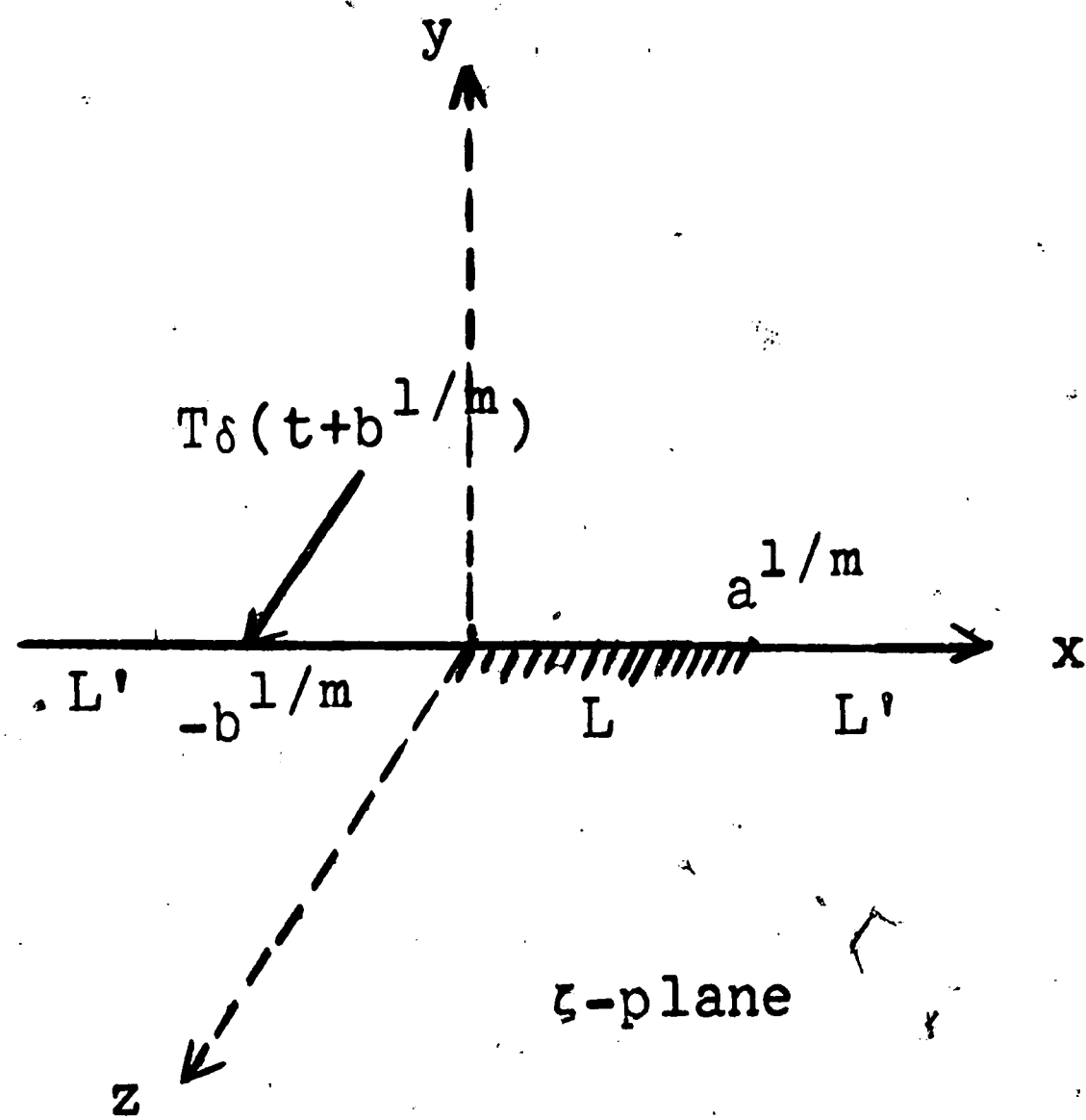


Fig. 8

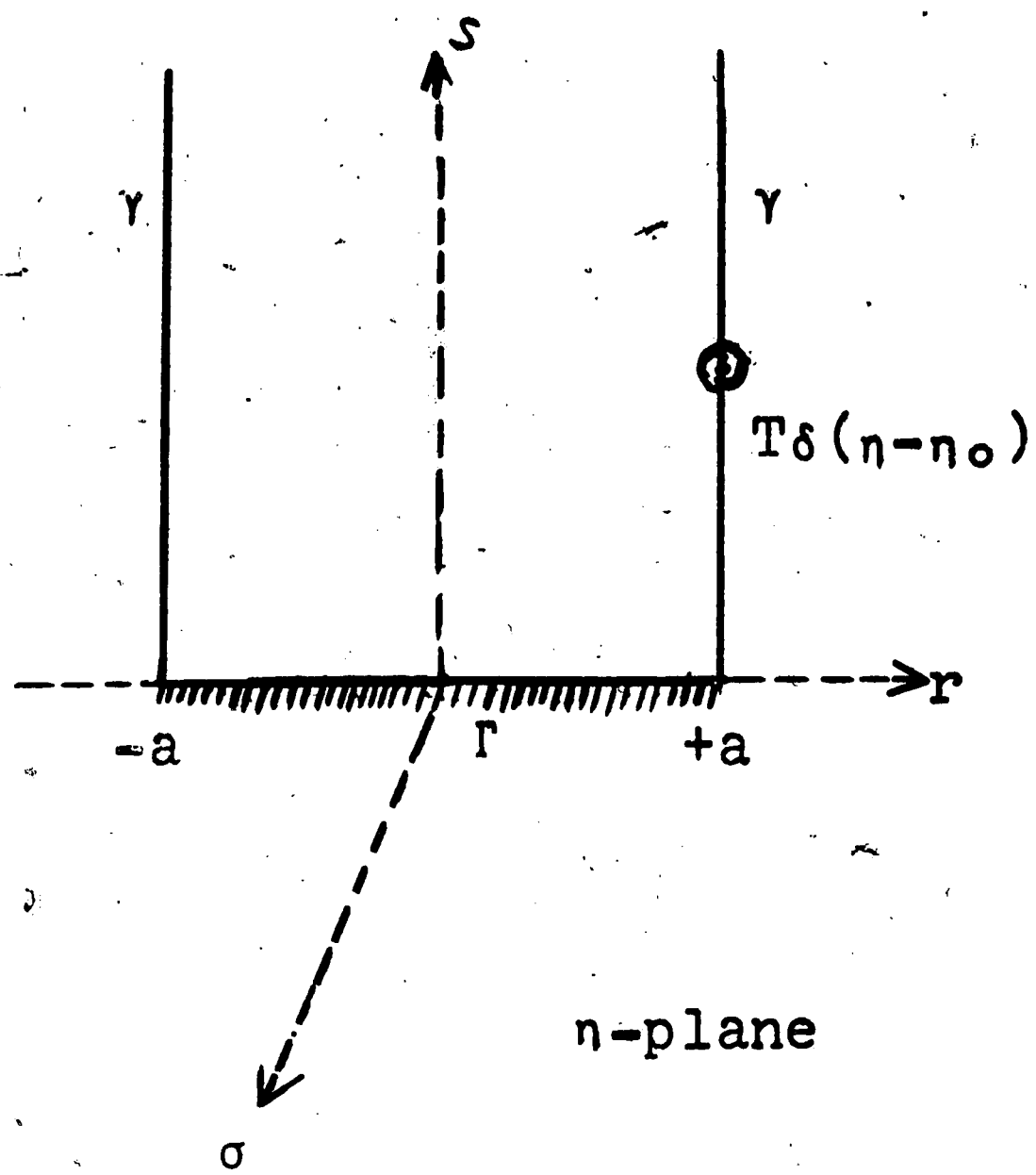


Fig. 9

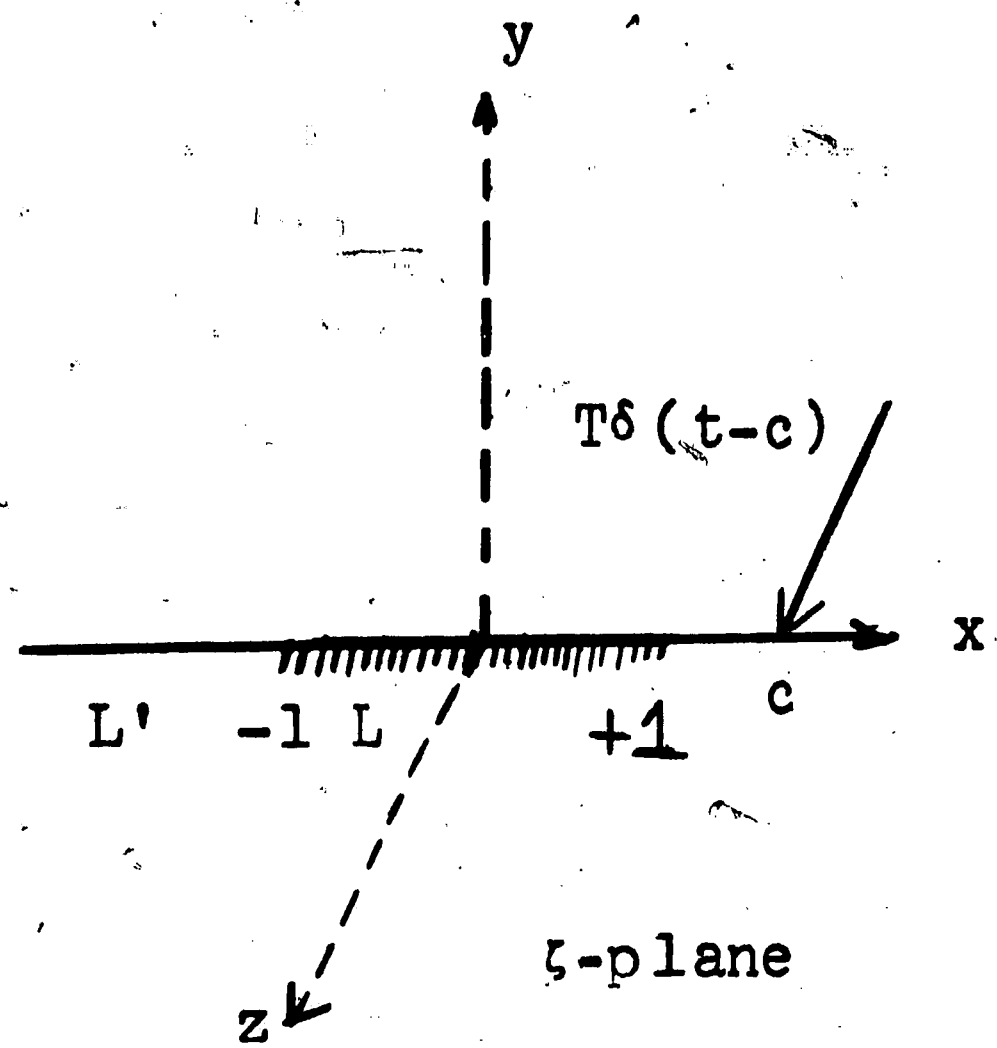


Fig. 10

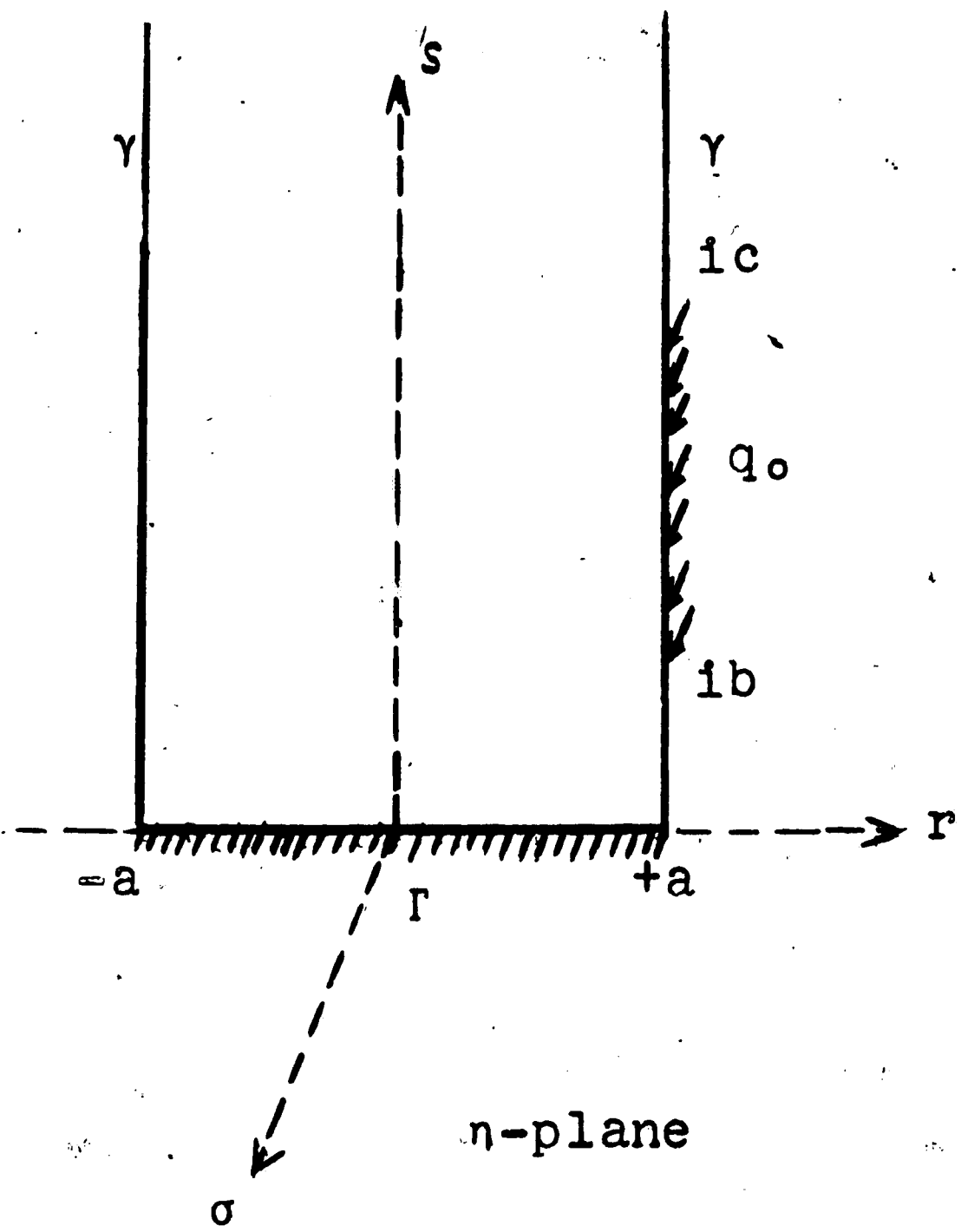


Fig. 11

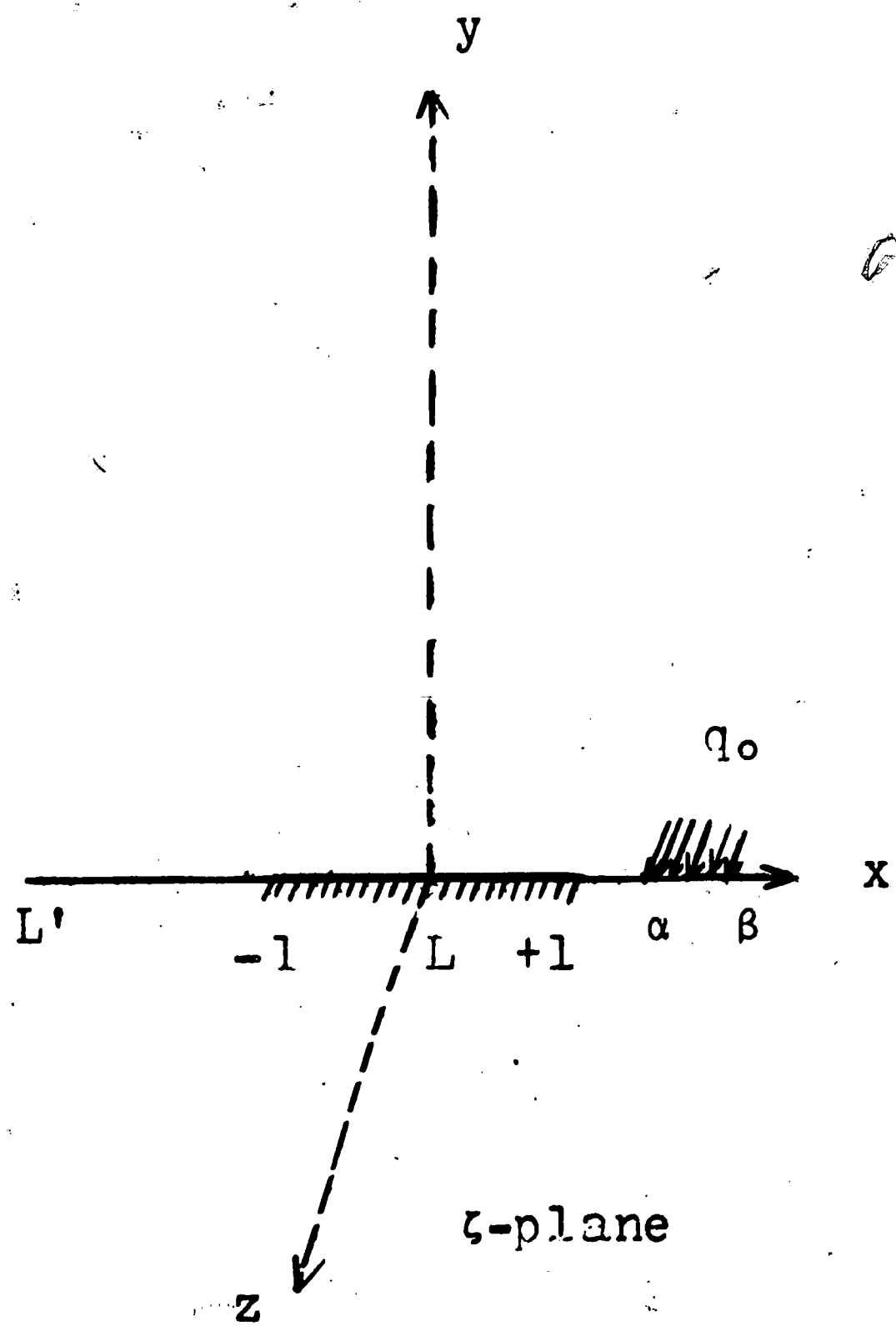


Fig. 12

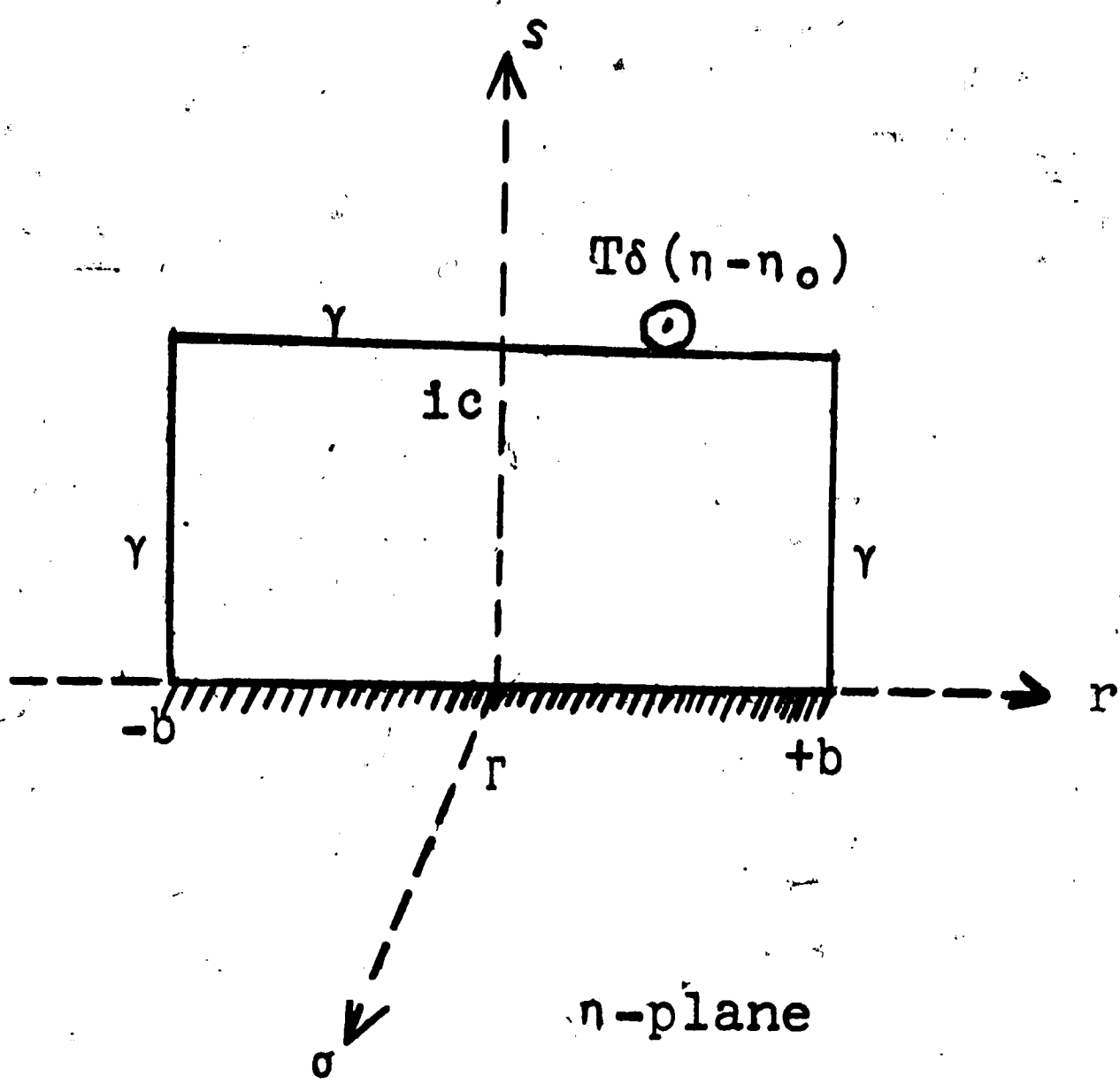


Fig. 13

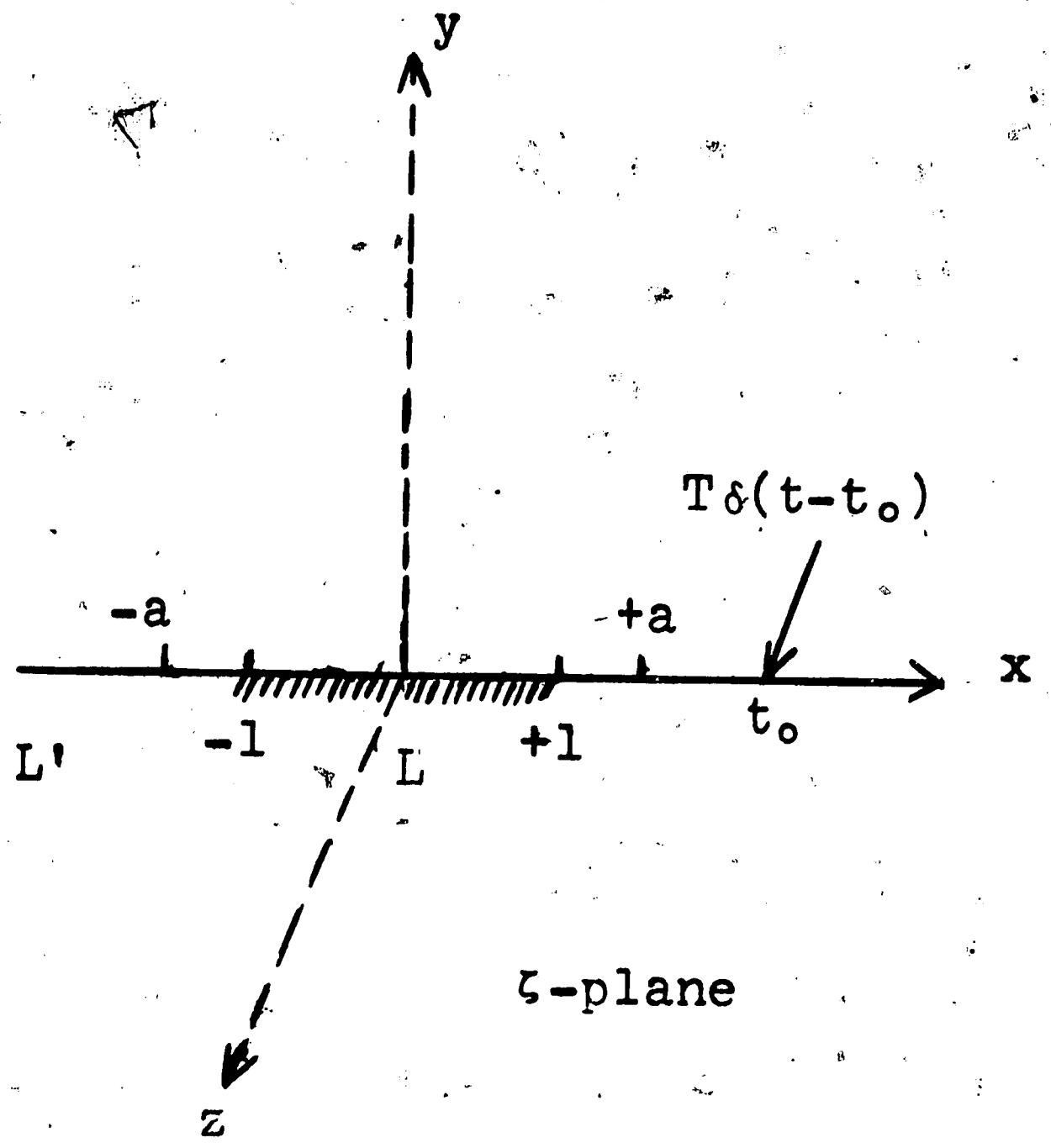


Fig. 14

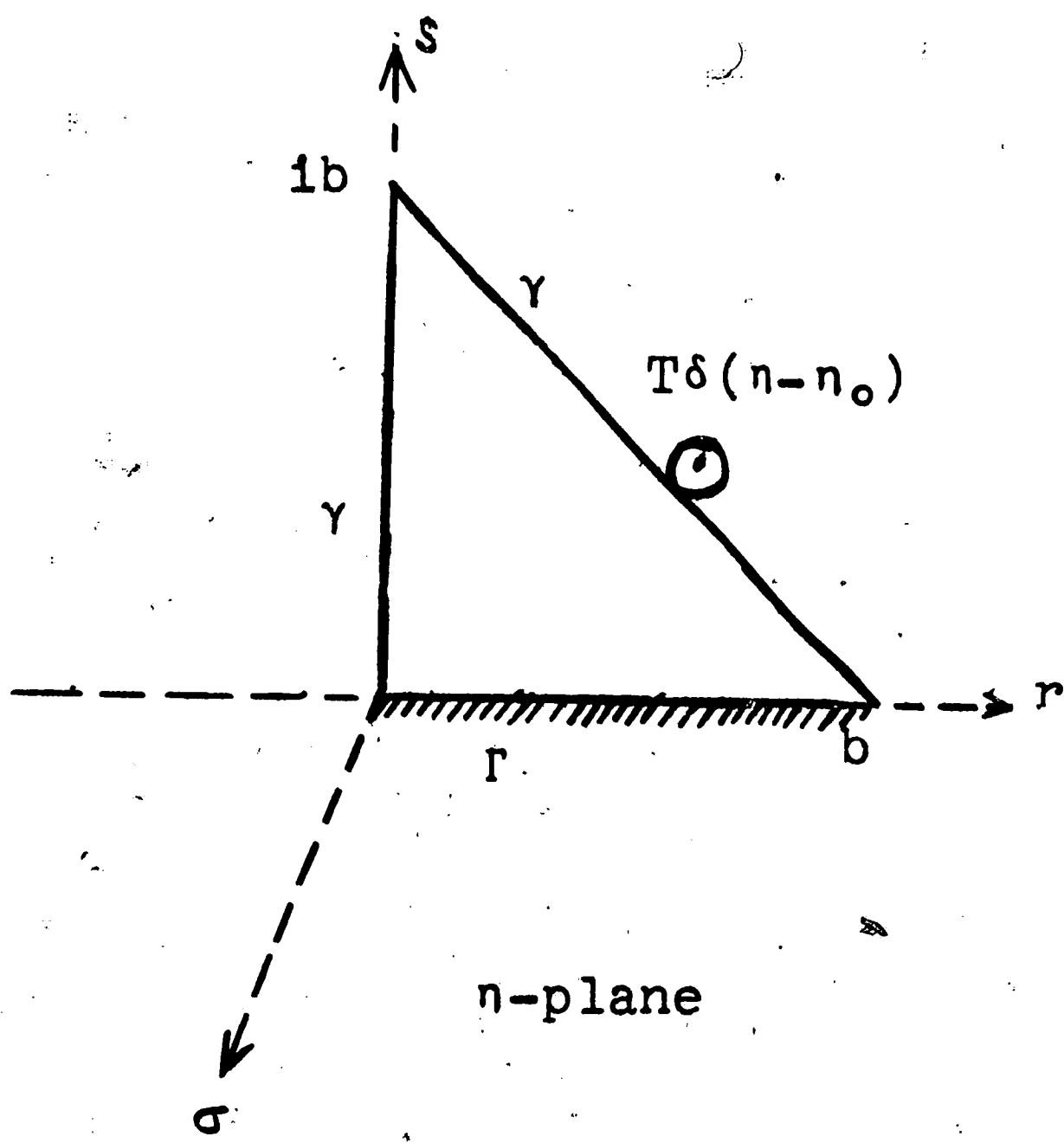


Fig. 15

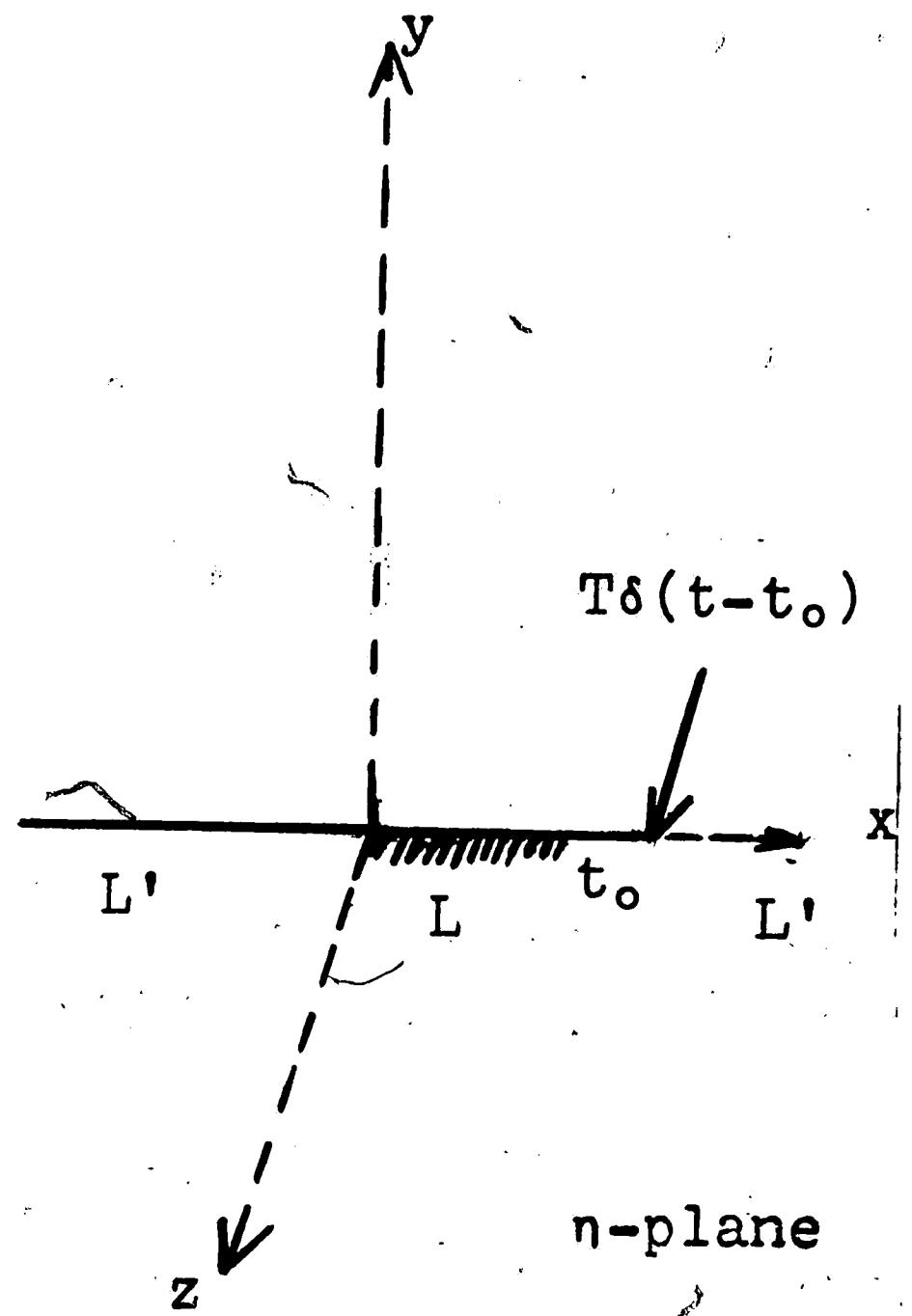


Fig. 16

Fig. 17

x vs. α from Table I

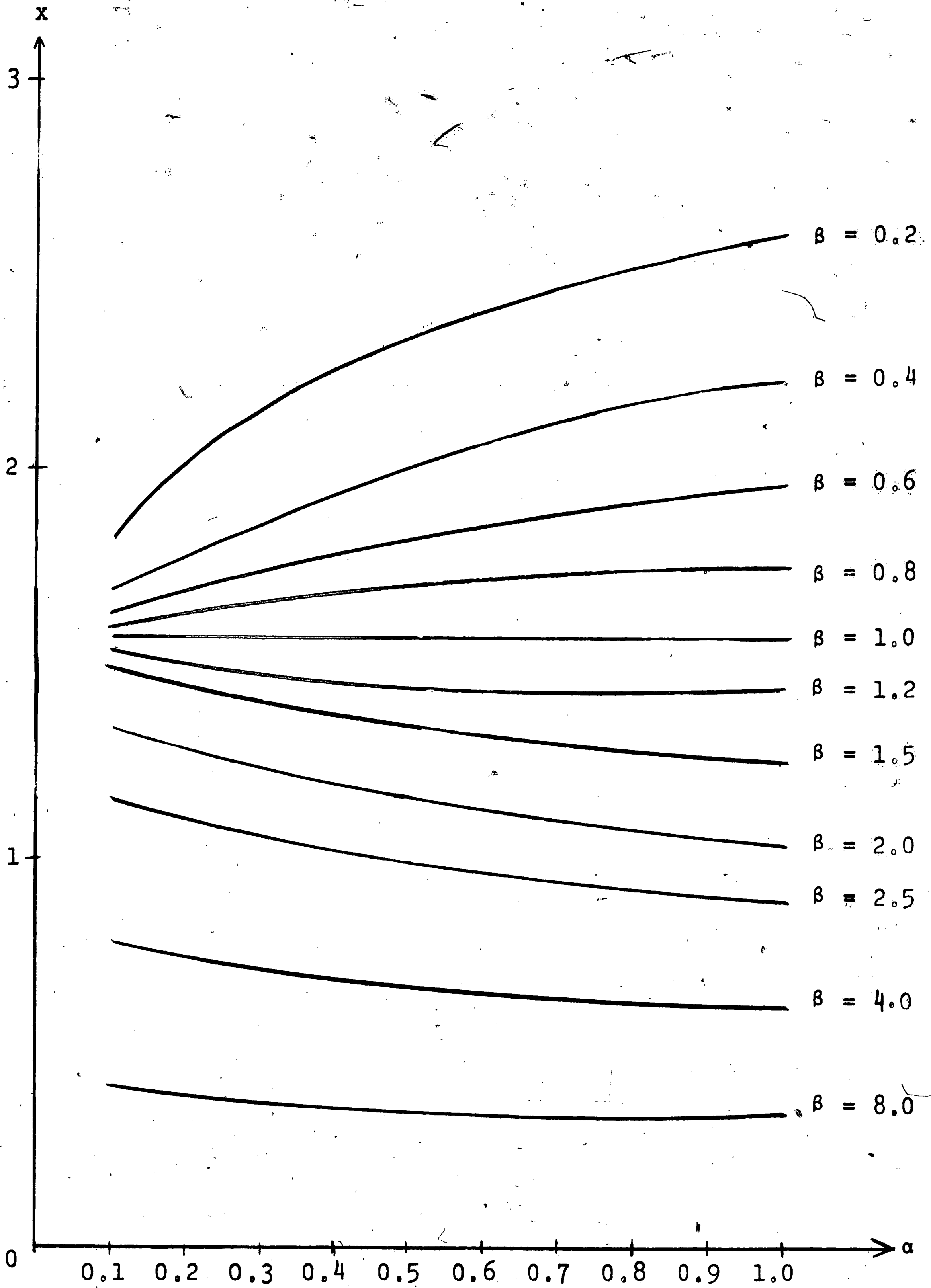


Fig. 18
x vs. α from Table II

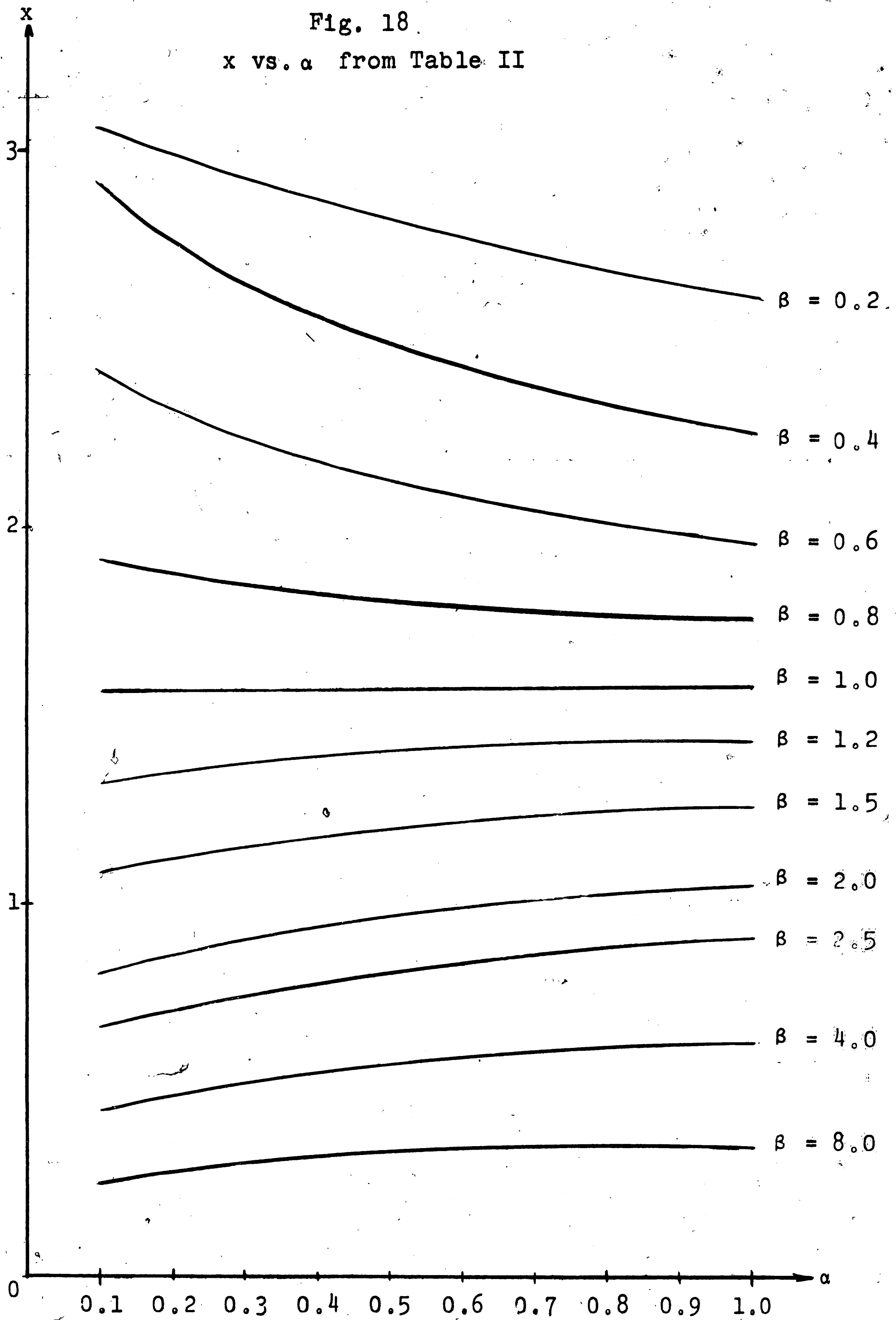
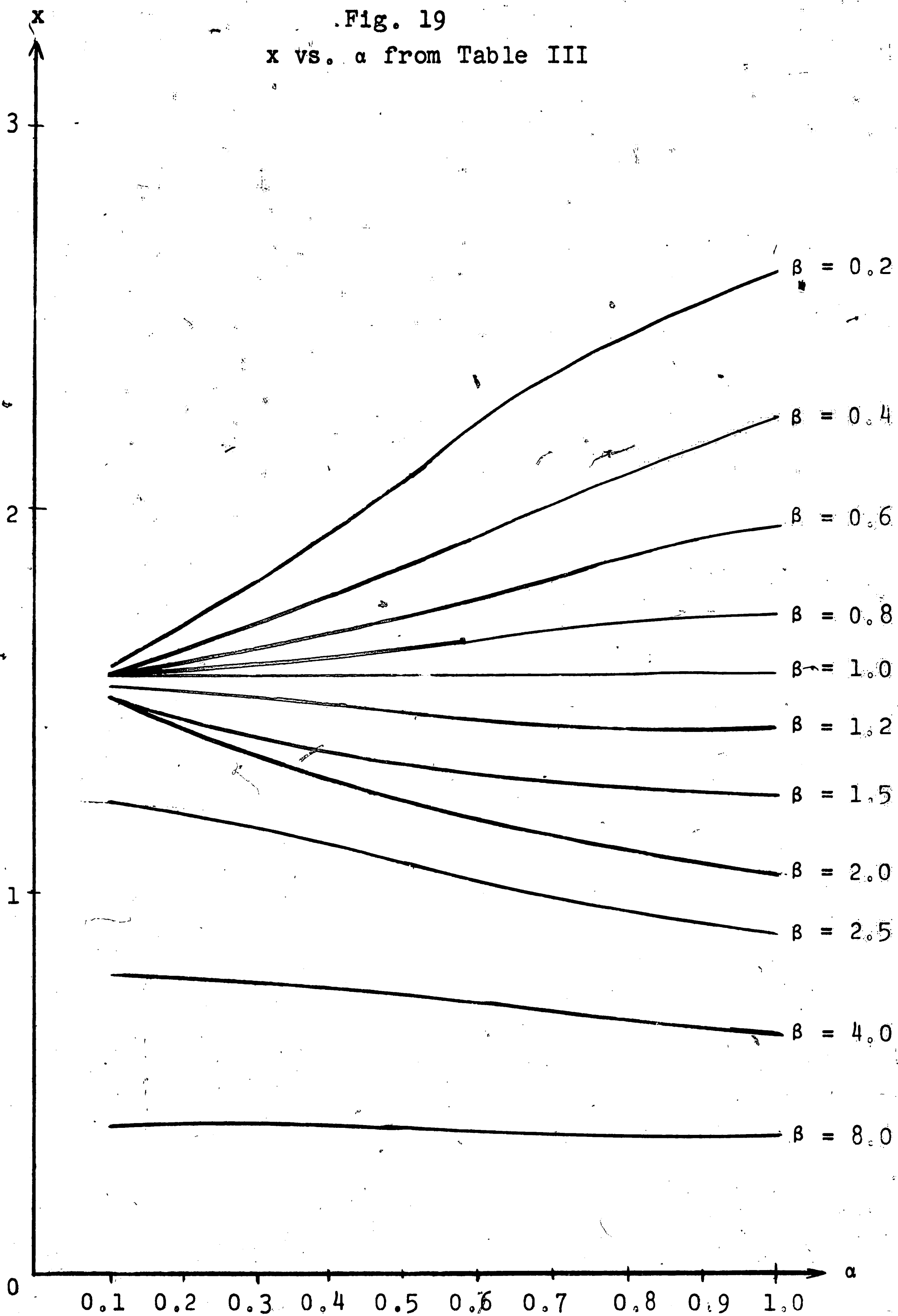


Fig. 19
x vs. α from Table III



References

- [1] G.R. Irwin, Handbuch der Physik, vol.6, Springer, Berlin (1958)
- [2] G.I. Barenblatt, Advances in Applied Mechanics, 7, 55-129 (1962)
- [3] N.I. Sneddon, Crack Problems in the Mathematical Theory of Elasticity, North Carolina State College, Raleigh (1961)
- [4] M.L. Williams, Bulletin of the Seismological Society of America, 49, 199-204 (1959)
- [5] A.R. Zak and M.L. Williams, Journal of Applied Mechanics, 30, 142-143 (1963)
- [6] F. Erdogan, Journal of Applied Mechanics, 30, 232-236 (1963)
- [7] F. Erdogan, (to be presented in 1965 Winter ASME meeting in New York and published in the Journal of Applied Mechanics, 1965)

- [8] G.I. Barenblatt and G.P. Cherepanov, PMM, 25, 1654-1666, (1961)
- [9] F. Erdogan, Bonded Dissimilar Materials Containing Cracks and Cavities Under Longitudinal Shear.
(Obtained in the course of research supported by a grant from NSF (GP-3200) (not published)
- [10] N.I. Muskhelishvili, Singular Integral Equations, P. Noordhoff N.V. - Groningen - Holland (1953)

Vita

The author was born February 3, 1942 to Allen B. and Hilda J. Ballard of Philadelphia, Pennsylvania.

His education began in the Philadelphia school system and he graduated from them in January 1960. Upon graduating Germantown High School he received a four year Philadelphia Board of Education Scholarship to the University of his choice and another scholarship from Lehigh University. He entered Lehigh University in September, 1960 and graduated from the same in June 1964. He married the former Miss Geraldine Floyd on May 30, 1964.

He began graduate study at Lehigh University under a National Science Foundation Traineeship in September, 1964. He expects to be awarded the Master of Science Degree in applied mechanics in October, 1965.

He began employment in June, 1965, with the International Business Machines Corporation, Glendale Development Laboratory, in Endicott, New York.